1) Please move Table S5 and add information

We have done this

2) Fig 2: Do we have stable isotope data from the stream/river?

Fig 2 does not incorporate/include data on stream/river water because the samples used in Fig 2 relate to GW isotopes only, and these are labelled as such (i.e. bore water). None of the trees sampled were close to water in a river/stream.

3) Fig 3 please show *E. camaldulensis* and *C. opaca* as different colours

We have done this

4) Figs 6, 7 please show *E. camaldulensis* and *C. opaca* as different colours

We have done this

5) p 31 line 1 – correct the omission of the phrase "differences in"

We have done this

6) Replace "Mulga" with A*c*acia spp.

We have done this

7) Map in the supplementary material is missing and numbers 1 – 4 definition.

Map is contained in the supplementary material and no numbers 1 – 4 included.

8) Does vertical distance mean elevation?

Yes it does and we have defined the word vertical to mean elevation above the stream.

9) Correct the conclusion regarding distance, increases and decreases in Δ^{13}C and WUEi.

We have corrected the error in the conclusion.

Speculations on the application of foliar ^{13}C discrimination to reveal groundwater dependency of vegetation, provide estimates of root depth and rates of groundwater use

Rizwana Rumman[1], James Cleverly[1], Rachael H. Nolan[1], Tonantzin Tarin[1] and Derek Eamus[1,2]

[1]Terrestrial Ecohydrology Research Group

School of Life Sciences

University of Technology Sydney

PO Box 123

Broadway

NSW 2007

Australia

Correspondence to: Derek Eamus (Derek.Eamus@uts.edu.au)

Abstract.

Groundwater-dependent vegetation is globally distributed, having important ecological, social and economic value. Along with the groundwater resources upon which it depends, this vegetation is under increasing threat through excessive rates of groundwater extraction.

In this study we examined one shallow-rooted and two deep-rooted tree species at multiple sites along a naturally occurring gradient in depth-to-groundwater. We measured (i) stable isotope ratios of leaves (δ^{13}C), xylem and groundwater (δ^2H and δ^{18}O); and (ii) leaf vein density. We established that foliar discrimination of ^{13}C (Δ^{13}C) is a reliable indicator of groundwater use by vegetation and can also be used to estimate rooting depth. Through comparison with a continental-scale assessment of foliar Δ^{13}C, we also estimated the upper limits to annual rates of groundwater use. We conclude that maximum rooting depth for both deep-rooted species ranged between 9.4 m and 11.2 m and that annual rates of groundwater use ranged *ca* 1400 – 1700 mm for *Eucalyptus camaldulensis* and 600 – 900 mm for *Corymbia opaca*. Several predictions about hydraulic and leaf traits arising from the conclusion that these two species made extensive use of groundwater were supported by additional independent studies of these species in central Australia.

1 Introduction

Drylands cover 41% of the earth's total land area (Reynolds et al., 2007) and are sub-categorized as hyper-arid, arid, semi-arid and dry sub-humid areas. Hyper-arid, arid and semi-arid regions are characterized by chronic water shortage with unpredictable rainfall (Clarke, 1991). Approximately 40 % of the world's population reside in drylands and groundwater represents a major water resource both for human consumptive use but also for groundwater dependent ecosystems (GDEs' Eamus et al., 2005). Sustainable management of both groundwater

and GDEs requires identification of the location of GDEs, rooting depth of vegetation and rates of groundwater use but attaining such information present significant technical and cost challenges (Eamus et al., 2015).

Approximately 70% of Australia is classified as semi-arid or arid (Eamus et al., 2006; O'Grady et al., 2011). Furthermore, annual potential evaporation exceeds annual rainfall across most of the continent, thus most Australian biomes are water-limited according to the Budyko (1974) framework (Donohue et al., 2009). On average, central Australia receives less than 350 mm y^{-1} of rainfall, making water a primary limiting resource (Eamus et al., 2006). Because surface water bodies in this region are mostly ephemeral (NRETAS, 2009, although see Box et al., 2008, regarding the small number of permanent water bodies), groundwater plays an important role in maintaining ecosystem structure and function of terrestrial (especially riparian) vegetation (Eamus et al., 2006). Owing to the remoteness of much of Australia's interior, few studies have investigated groundwater use by vegetation communities in these semi-arid regions.

Stomatal conductance is regulated to maximise carbon gain whilst simultaneously minimising transpiration (Cowan and Farquhar, 1977; Medlyn et al., 2011) and is sensitive to both soil and atmospheric water content (Prior et al., 1997; Thomas and Eamus, 1999). Intrinsic water-use efficiency (WUE_i), defined by the ratio of carbon gain to stomatal conductance) provides valuable insights on how vegetation responds to variation in water availability (Beer et al., 2009). Declining water supply results in increased WUE_i as stomatal conductance declines (Eamus et al., 2013). Discrimination against the ^{13}C isotope ($\Delta^{13}C$) is commonly used to calculate WUE_i. $\Delta^{13}C$ provides a time-integrated measure of WUE_i (Cernusak et al., 2011); in this study we examined spatial and seasonal patterns in $\Delta^{13}C$ across three tree species in the Ti Tree basin.

The present study was undertaken in the Ti Tree basin, which is the location of an important groundwater resource in central Australia (Cook et al., 2008a). Rainfall occurs mostly in large events during the austral summer (Dec – Mar); thus there is minimal rainfall available for vegetation use over prolonged periods. The dry-season in this region is characterized by declining soil water availability and high vapour pressure deficits (Eamus et al., 2013). Previous studies have documented several surprising attributes for a number of tree species in the Ti Tree. O'Grady et al.,. (2009) observed that, despite living in an extremely water limited environment, the specific leaf-area (SLA) of *Corymbia opaca* and *Eucalytptus camaldulensis* were similar more to those from highly mesic environments than to species from arid environments. Similarly, Santini et al.,. (2016) observed that xylem wall thickness and vessel implosion resistance were significantly smaller in *E. camaldulensis* and *C. opaca* than in shallow-rooted *Acacia aneura*. Finally, differences in rates of water use and changes in midday water potential between the end of the wet-season and the end of the dry-season were minimal for *E. camaldulensis* and *C. opaca* but were very large for *Acacia aptaneura* (which was previously classified as *Acacia aneura*; Maslin and Reid, 2012; Nolan et al., 2017). *A. aneura* and *A. aptaneura* often intermix with other members of the large Mulga complex of closely related *Acacia* species (Wright et al., 2016), thus we will refer *Acacia* spp. in the Mulga complex by the primary type, *A. aneura*. *A. aneura* is shallow-rooted and associated with shallow hard pans in this catchment (*ca* 1 m below ground surface; Cleverly et al., 2016a; Cleverly et al., 2016b) which prevents access to the groundwater below. *E. camaldulensis* is a riparian species, confined to narrow corridors along the ephemeral streams in the Ti Tree (the Woodforde River and Allungra Creek) where groundwater depth is shallow (< 3m); *C. opaca* is deep- rooted and may access groundwater to

depths of 8 m or more (O'Grady et al., 2009). These observations lead to the first hypothesis tested in the present study: that WUE_i of *A. aneura* would be significantly larger than that of *E. camaldulensis* and *C. opaca* because reliance on shallow stores of water by *Acacia* spp. imposes severe restrictions on water use, thus resulting in a large WUE_i.

5   Vertical (i.e. elevation) and horizontal distance from rivers receiving groundwater inflows in arid-zones influences the degree to which trees access groundwater (O'Grady et al., 2006a; Thorburn et al., 1994). Trees closest to the river (i.e. elevationally and horizontally) have xylem water deuterium and ^{18}O isotope ratios (δ^2H and $\delta^{18}O$, respectively) that are close to the ratios of river and groundwater; trees further from the river have xylem water ratios increasingly different from those of groundwater and the river (O'Grady et al., 2006a). In

10   endoreic basins like Ti Tree, evaporation of near-surface soil water imposes additional fractionation of δ^2H and $\delta^{18}O$ (Craig, 1961) relative to groundwater, thus δ^2H and $\delta^{18}O$ in xylem provides information on plant water source and climate (Cullen and Grierson, 2007). Variation in plant water sources with distance from the river can affect stomatal conductance and WUE_i. In this study we tested the hypothesis that WUE_i would increase with distance from the creek.

15   Differential access to water among co-occurring species within a biome results in variation of several morphological traits, including SLA (Warren et al., 2005), Huber value (Eamus et al., 2000; Sperry, 2000) and wood density (Bucci et al., 2004; Hacke et al., 2000). Leaf vein density (LVD) is a trait that influences whole-plant performance. From a resource investment perspective, leaves are composed primarily of two components: mesophyll that undertakes photosynthesis and a leaf-vein network which delivers water and nutrients to the leaf.

20   Investment in leaf veins is underpinned by resource allocation strategies (Niinemets et al., 2007; Niinemets et al., 2006; Niklas et al., 2007). Leaf-vein density is responsive to several environmental variables, but especially aridity (Uhl and Mosbrugger, 1999). Furthermore, LVD is positively correlated with leaf hydraulic conductance (K_{leaf}), maximum photosynthetic rate and leaf-level gas-exchange rates (Brodribb et al., 2007; Sack et al., 2003; Sack and Frole, 2006; Sack and Holbrook, 2006). Consequently we investigate whether investment in LVD of

25   three dominant overstorey tree species was affected by increasing depth-to-groundwater (DTGW).

The propensity for leaves to lose water matches the capacity of xylem to deliver the same volume of water (Brodribb and Holbrook, 2007; Meinzer and Grantz, 1990; Sperry, 2000), and positive correlations consequently occur between leaf-hydraulic conductance (K_{leaf}) and LVD (Brodribb et al., 2007; Sack and Holbrook, 2006). LVD provides a direct estimate of K_{leaf} because it correlates with the distance water must traverse from termini

30   of the xylem-network to sites of evaporation (Brodribb et al., 2010). Since transpiration is directly linked to availability of water to roots, we hypothesised that LVD will be correlated with depth-to-groundwater in plants for which groundwater is accessible; this correlation should be absent in species with shallow roots which cannot access groundwater. Whilst a number of studies have demonstrated increased LVD with increasing aridity along rainfall gradients (Brodribb et al., 2010; Brodribb and Holbrook, 2003; Sack and Holbrook, 2006),

35   this relationship has not, to our knowledge, been examined in relation to DTGW. Finally, because LVD is strongly correlated with K_{leaf} and rates of leaf-scale gas exchange (Brodribb et al., 2007; Sack et al., 2003; Sack and Frole, 2006), we hypothesise that LVD will be significantly correlated with $\Delta^{13}C$ (and hence WUE_i).

To summarize, we address the following questions:

1. Does access to groundwater by *E. camaldulensis* and *C. opaca* result in significantly smaller WUE_i compared to *A. aneura*?
2. Does LVD correlate with DTGW in the three species examined?
3. Is there a correlation between LVD and $\Delta^{13}C$ (and hence WUE_i) for the three species examined?
4. Does horizontal and vertical (i.e. elevational) distance from a known river flood-out zone influence foliar $\Delta^{13}C$ and WUE_i of co-occurring species?
5. Can foliar $\Delta^{13}C$ be used as an indicator of utilisation of groundwater by vegetation of arid regions?
6. Can foliar $\Delta^{13}C$ be used to estimate rooting depth and upper and lower bounds of rates of groundwater use?

2 Materials and methods

2.1 Site description

The study was conducted in the Ti Tree Basin, a 5500 km^2 basin located approximately 200 km north of Alice Springs NT and 180 km north of the Tropic of Capricorn (22.28°S, 1933.25°E, 549 m asl). Climate is characterized as tropical and arid with hot summers and warm winters. The nearest Bureau of Meteorology station (Territory Grape Farm; Met Station 015643; within 25 km of all study sites) recorded mean and median annual precipitation of 319.9 and 299 mm, respectively (1987 - May 2016; http://www.bom.gov.au/). Of the annual median rainfall, 72% falls during the summer months (December - February) and 86% falls during the monsoon season (November - April). Mean minimum and maximum monthly temperatures range from 5°C and 22.6°C in July to 22°C and 37.5°C in January.

The soil is a "red kandosol" (74:11:15 sand: silt: clay; Eamus et al., 2013), typical of large portions of semi-arid Australia, and has a high potential for drainage (Morton et al., 2011; Schmidt et al., 2010). Patches of hard siliceous soil is often observed and are likely surface expressions of the underlying hardpan (Cleverly et al., 2013), a common formation in the top 1 – 1.5 m in this type of soil (Cleverly et al., 2013; Cleverly et al., 2016a; Cleverly et al., 2016b; Morton et al., 2011). The major potable source of water for this region is a large underground reservoir, recharged mainly by seepage from creek/river channels and their flood-out zones, "mountain" front recharge and by occasional very heavy rainfall events (NRETAS, 2009; Calf et al., 1991). The Ti Tree basin has a natural gradient in DTGW. The depth of the water table below ground level is shallow (< 2m) in the northern part and groundwater is lost through evapotranspiration (Shanafield et al., 2015), whereas DTGW reaches 60 m in the southern and western part of the basin and 20 – 40 m in the eastern region (NRETA, 2007).

All study sites were characterized as being in one of three distinct vegetation types (Nolan et al., 2017; Cleverly et al., 2016a): (1) riparian, predominantly consisting of *Eucalyptus camaldulensis var. obtusa*, which line the banks of the ephemeral streams in the Ti Tree basin (Woodforde River and Allungra Creek); (2) low mixed woodland (*A. aneura* F.Muell. ex Benth., *A. aptaneura* Maslin & J.E.Reid, *A. kempeana* F.Muell.) with an

5

understorey of shrubs, herbs and C_3 and C_4 grasses; (3) tall, open *Corymbia* savanna with extensive Spinifex grass (*Triodia spp.*), sparse *Corymbia opaca* (D.J.Carr & S.G.M.Carr) K.D.Hill & L.A.S.Johnson trees and occasional *Acacia* spp. trees. The Woodforde River and Allungra Creek are ephemeral streams that flow only after large extensive rainfall events.   Nonetheless, perched aquifers beneath their riparian corridors are
5   recharged by large storms (Villeneuve et al., 2015), providing long-term access to groundwater near ephemeral streams. Allungra Creek and its flood-out zone represent zones of local recharge (NRETAS 2009). Overbank flooding and sheet flow occur in flood-outs where the Woodforde River and Allungra Creek enter the basin and split into a network of smaller channels (NRETA, 2007), resulting in an estimated 1.8 ML of groundwater recharge per year (NRETAS, 2009).

10   Four sampling plots were established for determination of foliar $\Delta^{13}C$ and of $\delta^{18}O$ and δ^2H values for xylem water and groundwater from a nearby bore. DTGW in each of the four plots was 4.4 m, 8.3 m, 8.8 m and 13.9 m, respectively. One of the four plots was located on the banks of the Woodforde River (plot 1, DTGW = 4.4 m). *E. camaldulensis* is the dominant tree species in plot 1, and *C. opaca* is also present. In the second plot, *A. aneura* is the dominant species (plot 2, DTGW = 8.3 m). *C. opaca* is the dominant tree species in the two
15   remaining plots (plot 3, DTGW = 8.8 m; plot 4, 13.9 m).

$\Delta^{13}C$ of *E. camaldulensis*, *C. opaca* and *A. aneura* were examined along three additional transects to investigate the influence topography and of distance from a creek on WUE_i. The three transects established perpendicular to the banks of Allungra Creek, which is in an area of known groundwater recharge at the base of the hills that bound the southern extent of the basin (NRETAS, 2009). One of the three transects was located near a
20   permanent waterhole near the flood-out and the bottom of Allungra Creek. Transects two and three were 1 – 2 km upstream of the water hole. Transects extended from the shore within 1 m of the creek up to a maximum of 1800 m from the creek (vertical i.e elevational, distance from the creek bed ranged 0 – 4 m; Supplementary Fig S2a –c), across which vegetation graded from riparian forest to *Corymbia* open savanna, with occasional *Acacia* spp. trees interspersed throughout.

25   In addition to the four plots and three transects, "spot sampling" for foliar $\Delta^{13}C$ alone was performed at three sites to extend the examination of variation in WUE_i to   20 m, 36 m and 49.5 m DTGW for *A. aneura* or 20 m and 36 m for *C. opaca*. Finally, continental sampling of foliar $\Delta^{13}C$ of multiple dominant tree species was undertaken at seven sites distributed across Australia (Rumman et al., 2017) (Table S1; Karan et al., 2016; Rumman 2017) in order to allow comparison of foliar $\Delta^{13}C$ of our three Ti-Tree species with a continental-scale
30   regression of $\Delta^{13}C$ with rainfall. A summary of the isotopes analysed for each species and for each groundwater sampling undertaken, for each site is given in Table 1.

2.2 Leaf sampling protocols and meteorology

Sampling was undertaken in April 2014 (end of wet-season) and September 2013 (end of dry-season). Three mature, healthy leaves on each of three branches from two or three replicate trees were sampled for $\Delta^{13}C$ in all
35   plots, transects and spot sampling sites. In addition, terminal branches of the trees in the four plots were collected for deuterium and $\delta^{18}O$ analyses of xylem water. Bore water samples were also collected in the four plots and the three spot sampling sites using a Groundwater samples were also collected from the bores located

at each site using HydraSleeve no-purge groundwater sampler (Cordry, 2003). Sampling along the three transects occurred at three or four points along each transect. The three trees of each of the dominant species at each location were located within 50 m of the bore. Leaves for leaf vein analysis (see below) were collected during Sept 2013.

5   Climate conditions preceding and during the sampling periods were obtained from two eddy-covariance towers (Fluxnet sites AU-ASM and AU-TTE; Cleverly et al., 2016a; Cleverly 2011; Cleverly 2013). AU-ASM is located to the west of the Ti Tree at the spot sampling site where DTGW is 49.5 m. AU-TTE is located near the eastern edge of the Ti Tree in plot 3 where DTGW is 8.8 m.

2.3 Stable isotope analyses: deuterium, $\delta^{18}O$ and foliar $\Delta^{13}C$

10   Branch xylem water was extracted by cryogenic vacuum distillation (whereby samples are subject to a vacuum and water vapour is frozen using liquid nitrogen, as described in Ingraham and Shadel, 1992; West et al., 2006). Water from each branch sample was extracted for a minimum of 60-75 minutes (West et al., 2006). δ^2H and $\delta^{18}O$ analyses of branch water and groundwater were performed using a Picarro L2120-i Analyser for Isotopic H_2O. Five laboratory standards were calibrated against IAEA VSMOW2 – SLAP2 scale (Vienna Standard Mean

15   Ocean Water 2, VSMOW2: $\delta^{18}O$ = 0 ‰ and δ^2H = 0 ‰; Standard Light Antarctic Precipitation 2, SLAP2: $\delta^{18}O$ = -55.5 ‰ and δ^2H = -427.5 ‰) and Greenland Ice Sheet Precipitation (GISP, $\delta^{18}O$ = -24.8 ‰ and δ^2H = -189.5 ‰) as quality control references (IAEA, 2009). The standard deviation of the residuals between the VSMOW2 – SLAP2 value of the internal standards and the calculated values based on best linear fits was ca 0.2 ‰ for $\delta^{18}O$ and ca 1.0 ‰ for δ^2H.

20   **2.4 Carbon isotope ratios of leaves**

Leaf samples stored in paper bags were completely dried in an oven at 60℃ for five days. After drying, each leaf sample was finely ground to powder with a Retsch MM300 bead grinding mill (Verder Group, Netherlands) until homogeneous. Between one and two milligrams of ground material was sub-sampled in 3.5 mm X 5 mm tin capsules for analysis of the stable carbon isotope ratio ($\delta^{13}C$), generating three representative independent

25   values per tree. All $\delta^{13}C$ analyses were performed in a Picarro G2121-i Analyser (Picarro, Santa Clara, CA, USA) for isotopic CO_2. Atropine and acetanilide were used as laboratory standard references. Results were normalised with the international standards sucrose (IAEA-CH-6, $\delta^{13}C_{VPDB}$ = -10.45 ‰), cellulose (IAEA-CH-3, $\delta^{13}C_{VPDB}$ = -24.72 ‰) and graphite (USGS24, $\delta^{13}C_{VPDB}$ = -16.05 ‰). Standard deviation of the residuals between IAEA standards and calculated values of $\delta^{13}C$ based on best linear fit was ca 0.5 ‰.

30   **2.5 Calculation of WUE$_i$ from $\delta^{13}C$ and hence $\Delta^{13}C$**

WUE$_i$ was determined from ^{13}C discrimination ($\Delta^{13}C$), which is calculated from bulk-leaf carbon isotope ratio ($\delta^{13}C$), using the following equations (Werner et al., 2012):

$$\Delta^{13}\text{C (‰)} = \frac{R_a - R_p}{R_p} = \frac{\delta^{13}C_a - \delta^{13}C_p}{1 + \frac{\delta^{13}C_p}{1000}} \qquad (1)$$

$$WUE_i = \frac{c_a(b - \Delta^{13}\text{C})}{1.6(b - a)} \qquad (2)$$

2.6 Leaf vein density

A small sub-section (approximately 1 cm^2) of all leaves sampled for ^{13}C were used for LVD analysis, providing three leaf sub-sections per tree, nine samples per species. Due to the small size of *A. aneura* phyllodes, several phyllodes were combined and ground for ^{13}C analysis and one whole phyllode was used for LVD analysis. Each leaf section was cleared and stained following the approach described in Gardner (1975). A 5% (w/v) NaOH solution was used as the principal clearing agent. Leaf-sections were immersed in the NaOH solution and placed in an oven at 40℃ overnight (Gardner, 1975). Phyllodes of *Acacia* proved difficult to clear effectively and were kept in the oven longer than overnight to aid clearing. Once cleared, the partially translucent leaf sections were stained with a 1% (w/v) safranin solution. Most leaf sections were stained for up to three minutes and then soaked with a 95% (w/v) ethanol solution until the vein network was sufficiently stained and the majority of colour was removed from the lamina. After staining, the cuticle was removed to aid in identifying the vein network. Following cuticle removal, leaf sub-sections were photographed using a Nikon microscope (model: SMZ800) at 40 x magnification. Finally, minor veins were traced by hand and LVD was calculated as total vein length per unit area (mm/mm^2) using ImageJ version 1.48 (National Institutes of Health, USA).

2.7 Data and statistical analysis

Species-mean values (n = 9) for the dominant overstorey species at each location were calculated for δ^2H, δ^{18}O, δ^{13}C and LVD. Relationships between Δ^{13}C and WUE$_i$ with DTGW were tested using regression analysis after testing for non-normality (Shapiro-Wilk test, α = 0·05) and homogeneity of variances (Bartlett test). A Tukey's *post-hoc* test for multiple comparisons across sites was used to test for significance of variation as a function of DTGW. Breakpoints in functions with DTGW were determined using segmented regression analyses whereby the best fitting function is obtained by maximising the statistical coefficient of explanation. The least squares method was applied to each of the two segments while minimising the sum of squares of the differences between observed and calculated values of the dependent variables. Next, one-way ANOVA was applied to determine significance of regressions and breakpoint estimates within a given season. We fully acknowledge that the number of plots with shallow DTGW was sub-optimal, but constraints arising from species distribution across the TI-Tree precluded additional sampling.

3 Results

3.1 Meteorological conditions during the study period

Mean daily temperature and mean daily vapour pressure deficit (VPD) were largest in summer (December – February) and smallest in winter (June – August) (Figure 1). Daily sums of rainfall showed that the DTW 8.8 m and 49.4 m sites received 265 mm and 228 mm rainfall, respectively, between the September 2013 and April 2014 sampling dates, representing more than 73% and 60% of the total respective rainfall received from January 2013 to June 2014 at these sites.

3.2 Variation in source-water uptake

Xylem water isotope ratios for *A. aneura* were widely divergent from the bore water stable isotope ratios (Fig. 2a) in both wet and dry-seasons, indicative of lack of access to groundwater. In contrast, δ^2H and $\delta^{18}O$ of xylem water in *E. camaldulensis* and *C. opaca* were predominantly (with two exceptions) tightly clustered around δ^2H and $\delta^{18}O$ of groundwater in the bores located within 50 m of the trees (Fig. 2b). There was little variation in xylem water composition between the end of the dry and end of the wet-seasons for either species, reflecting the consistent use of groundwater by these two species.

$\Delta^{13}C$ of *A. aneura*, sampled in the *Corymbia* savanna and Ac*a*cia spp. plots was not significantly correlated with DTGW, in either season or across all values of DTGW (ANOVA F = 1.78; p > 0.05; Fig. 3a, b). As a consequence of these patterns in $\Delta^{13}C$, WUE_i did not vary significantly for *A. aneura* across sites differing in DTGW (Fig. 4a) despite the large variability in WUE_i (ranging 62 – 92 µmol mol^{-1}) across sites and seasons. By contrast, foliar $\Delta^{13}C$ of *E. camaldulensis* and *C. opaca* declined significantly with increasing DTGW in both seasons at the sites where DTGW was relatively shallow (DTGW < *ca* 12 m). Segmented regression analysis shown in Figure 3 (c) and (d) yielded breakpoints at 11.17 ± 0.54 m in September (ANOVA F = 11.548; df = 2, 38; P < 0.01) and 9.81 ± 0.4 m in April (ANOVA F = 14.67; df = 2, 47; P < 0.01), which represent the seasonal maximum depths from which groundwater can be extracted by these species. Thus, WUE_i of *E. camaldulensis* and *C. opaca* was significantly smaller at the shallowest site than at sites with DTGW > 13.9 m (Fig. 4b) but did not differ significantly across the deeper DTGW range (13.9 – 49.5 m; Fig. 4b).

As distance from Allungra creek increased, foliar $\Delta^{13}C$ for both *E. camaldulensis* and *C. opaca* declined significantly (Fig. 5a), with concomitant increases in WUE_i (Fig. 5b). There was no significant relationship for $\Delta^{13}C$ nor WUE_i with distance from the creek for *A. aneura* (data not shown).

3.3 Leaf vein density

Leaf vein density (LVD) did not vary significantly with increasing DTGW for *A. aneura* (Fig. 6a), but a significant increase was observed for DTGW < *ca* 10 m in the two deep-rooted species (Fig. 6b). The break point for *E. camaldulensis* and *C. opaca* (Fig. 6b; 9.36 m ± 0.6 m; ANOVA F = 6.38; P<0.05) agreed well with the two previous estimates (cf Figs. 3 and 6), although again, constraints imposed by species distributions severely limited the number of samplings available at shallow DTGW sites. As with LVD and DTGW, no

relationship was observed between LVD and $\Delta^{13}C$ for *A. aneura* (Fig. 7a), but a significant linear decline in $\Delta^{13}C$ with increasing LVD was observed for *E. camaldulensis* and *C. opaca* (Fig. 7b).

4 Discussion

Analyses of stable isotopes of bore water (i.e groundwater) and xylem water across a DTGW gradient established that *A. aneura* adopted an "opportunistic" strategy of water use and was dependent on rainfall stored within the soil profile. This is consistent with previous studies, where *Acacia* spp. was shown to be very responsive to changes in upper soil moisture content, as expected given their shallow rooting depth and the presence of a shallow (< 1.5 m) hardpan below stands of *Acacia* spp. (Eamus et al., 2013; Pressland, 1975). Furthermore, very low predawn leaf-water-potentials (< -7.2 MPa; Eamus et al., 2016) and very high sapwood density (0.95 g cm^{-3}; Eamus et al., 2016) in *A. aneura* of the Ti Tree and which are strongly correlated with aridity, confirms that they rely on soil water without access to groundwater, consistent with the findings of Cleverly et al.,. (2016b). By contrast, analyses of stable isotopes in groundwater and xylem water of *E. camaldulensis* and *C. opaca* established their access to groundwater, as has been inferred previously because of their large rates of transpiration in the dry-season and consistently high (close to zero) predawn water potentials (Howe et al., 2007; O'Grady et al., 2006a; O'Grady et al., 2006b). Importantly, we observed no significant change in xylem isotope composition for these two deep-rooted species (*E. camaldulensis* and *C. opaca*) between the end of the wet-season and the end of the dry-season, further evidence of year-round access to groundwater at the shallowest DTGW sites.

One specific aim of the present study was to determine whether discrimination against ^{13}C ($\Delta^{13}C$) and resultant intrinsic water-use efficiency (WUE_i) could be used to identify access to groundwater. An increase in foliar $\Delta^{13}C$ represents decreased access to water and increasing WUE_i (Leffler and Evans, 1999; Zolfaghar et al., 2014; Zolfaghar et al., 2017). The shallow-rooted *A. aneura* did not show any significant relationship of $\Delta^{13}C$ with DTGW during either season. Consequently mean WUE_i showed no significant trend with increasing DTGW, consistent with the conclusion that *A. aneura* only accessed soil water during either season. In contrast, a breakpoint in the relationship between $\Delta^{13}C$ and DTGW was apparent between 9.4 m (derived from LVD results) and 11.2 m (derived from $\Delta^{13}C$ analyses) when data for the two species were combined. Where DTGW was larger than a threshold (DTGW > *ca* 12m), $\Delta^{13}C$ became independent of DTGW. Consequently, WUE_i increased significantly as DTGW increased to these thresholds (p < 0.001) but did not vary with further increases in DTGW. We therefore suggest that foliar $\Delta^{13}C$ (or WUE_i) can be used as an indicator of groundwater access by vegetation. $\Delta^{13}C$ is less expensive and easier to measure than stable isotope ratios of water (δ^2H and $\delta^{18}O$) in groundwater, soil water and xylem water. Furthermore, canopies are generally more accessible than groundwater. Globally, identification of groundwater-dependent ecosystems has been hindered by the lack of a relatively cheap and easy methodology (Eamus et al., 2015), thus $\Delta^{13}C$ shows great promise for identifying groundwater-dependent vegetation and ecosystems.

Whilst acknowledging the sub-optimal distribution of samples across the shallow DTGW range (< 10 m) from which break-points in regressions were calculated (Figs. 3, 6), which arose because of the natural distribution of trees across the basin, we can ask the question: are the speculated depths beyond which groundwater appears to

become inaccessible supported by other independent studies of Australian trees? Several analyses support our suggestion of a lower limit of approximately 12 m beyond which groundwater is inaccessible to vegetation in this basin. Eamus et al., (2015) present the results of a seven site (seven sites across the range 2.4 – 37.5 m DTGW), 18 trait, 5 species study and identify a breakpoint between 7 – 9 m. Similarly, two recent reviews identify lower limits to root extraction of groundwater of 7.5 m (Benyon et al., 2006) and 8-10 m (O'Grady et al., 2010) while Cook et al., (1998b) established a limit of 8 – 9 m for a Eucalypt savanna. We therefore conclude that our estimates of the limits to groundwater accessibility appear reasonable.

Figure 8 shows combined $\Delta^{13}C$ from four Australian studies (Miller et al., 2001; Stewart et al., 1995; Taylor, 2008; Rumman et al., 2017), including one continental-scale study of foliar $\Delta^{13}C$ (Rumman et al., 2017). A single regression describes the data of all four independent studies. Thus, when rainfall is the sole source of water for vegetation, $\Delta^{13}C$ is strongly correlated with annual rainfall. In contrast, the mean $\Delta^{13}C$ for *E. camaldulensis* and *C. opaca* do not conform to the regression (Fig. 8). It appears that *E. camaldulensis* in the Ti Tree "behaves" as though it were receiving approximately 1700 mm of rainfall, despite growing at a semi-arid site (*ca* 320 mm average annual rainfall). This represents the upper limit to groundwater use by this species, assuming a zero contribution from rainfall (which is clearly very unlikely). The upper limit to annual groundwater use for *C. opaca* was similarly estimated to be 837 mm (Fig. 8). If all of the water from rainfall is used by these two species (which is also very unlikely) then the lower limit to groundwater use is the difference between rainfall and the estimates derived from Figure 8, about 1380 mm for *E. camaldulensis* and 517 mm for *C. opaca*.

There are several independent estimates of annual tree water-use for these two species which provide a valuable comparison to the estimates made above. O'Grady et al.,. (2009) showed that annual water use by riparian *E. camaldulensis* in the Ti-Tree was approximately 1642.5 m^3 m^{-2} sapwood y^{-1}. Assuming an average tree radius of 20 cm, a sapwood depth of 2 cm and an average canopy ground cover of 25 m^2 per tree yields an annual water use of 1568 mm y^{-1}, encouragingly close to the estimate (1700 mm) derived from Figure 8. The estimate for annual water use by *C. opaca* from O'Grady et al (2009) is 837 mm, in reasonable agreement with the estimate from the average $\Delta^{13}C$ of *C. opaca* and the regression in Figure 8 (*ca* 900 mm). Because depth-to-groundwater for *C. opaca* is significantly larger (*ca* 8 -10 m) than that for *E. camaldulensis* (*ca* 2 - 4 m), the resistance to water flow imposed by the xylem's path length is larger for *C. opaca* than *E. camaldulensis* and therefore water-use may be expected to be smaller in the former than the latter, as observed.

Using an entirely different methodology from that used here, O'Grady et al., (2006c) estimated annual groundwater use by riparian vegetation on the Daly River in northern Australia to be between 694 mm and 876 mm, while O'Grady and Holland, (2010) showed annual groundwater use to range from 2 mm to > 700 mm in their continenal-scale review of Australian vegetation. Therefore our estimates based on $\Delta^{13}C$ appear reasonable. We conclude that (a) *E. camaldulensis* and *C. opaca* are accessing groundwater (because annual water use greatly exceeded annual rainfall); (b) $\Delta^{13}C$ can be used as an indicator of groundwater use by vegetation; and (c) $\Delta^{13}C$ can provide estimates of upper and lower bounds for the rate of ground water use by vegetation.

4.1 Patterns of carbon isotope discrimination and intrinsic water-use efficiency along Allungra creek transects

For the two deep-rooted species (*E. camaldulensis* and *C. opaca*), a significant decline in Δ^{13}C (and hence an increase in WUE$_i$) was observed with increasing distance from the creek (Fig. 5a, b). In contrast to the results of O'Grady et al.,. (2006c) for a steeply rising topography in the Daly River, this is unlikely to be attributable to increased elevation since the change in elevation was minimal across each entire transect (< 3 m), and even smaller near Allungra Creek where most of the change in Δ^{13}C was recorded. Therefore the cause of the change in Δ^{13}C with distance from the creek was most likely to be a function of the frequency with which trees receive flood water and hence the amount of recharge into the soil profile (Ehleringer and Cooper, 1988; Thorburn et al., 1994; Villeneuve et al., 2015; Singer et al., 2014). We therefore further conclude that foliar Δ^{13}C can be used as an indicator of access to additional water to that of rainfall, regardless of the source of that additional water (e.g., groundwater, flood recharged soil water storage, irrigation).

4.2 Leaf vein density across the depth-to-groundwater gradient

In our study, LVD was independent of DTGW for *A. aneura* but a break point (9.4 m) was apparent across the combined data of the two deep rooted species. Increased DTGW reflects a declining availability of water resources (Zolfaghar et al., 2015), especially in arid-zones. Uhl and Mosbrugger (1999) concluded that water availability is the most important factor determining LVD. Sack and Scoffoni (2013) also showed LVD to be negatively correlated with mean annual precipitation in a 796 species meta-analysis. Therefore increasing LVD with increasing DTGW is consistent with the positive effect of water supply on LVD, despite similar amounts of rainfall being received along the DTGW gradient.

Both *A aneura* and *C. opaca* in the present study showed LVDs close to the higher end of the global spectrum (Sack and Scoffoni, 2013), consistent with larger LVDs observed in "semi-desert" species. Higher LVDs allow for a more even spatial distribution of water across the phyllode or lamina during water-stress, which contributes to a greater consistency of mesophyll hydration in species of arid and semi-arid regions (Sommerville et al., 2012). In turn, this allows continued photosynthetic carbon assimilation during water-stress (Sommerville et al., 2010). Presumably, a large LVD also decreases the resistance to water flow from minor veins to mesophyll cells, which is likely to be beneficial for leaf hydration as water availability declines while also facilitating rapid rehydration following rain in these arid-zone species. Large LVDs for *A. aneura* of semi-arid regions in Australia have been associated with rapid up-regulation of phyllode function with the return of precipitation following drought (Sommerville et al., 2010), and such rapid up-regulation is crucial for vegetation in regions with unpredictable and pulsed rainfall like the Ti Tree (Byrne et al., 2008; Grigg et al., 2010).

LVD was negatively correlated with bulk-leaf Δ^{13}C (and thus positively correlated with WUE$_i$) in *C. opaca* and the data for *E. camaldulensis* appeared to conform to the regression for *C.opaca* (Fig. 7b). What mechanism can explain the significant relationship observed between a structural leaf-trait (LVD) and a functional trait (WUE$_i$)? The stomatal optimization model (Medlyn et al., 2011) is based on the fact that transpiration (E) and CO_2 assimilation (A) are linked via stomatal function. In order to gain carbon most economically while minimising water loss (i.e., optimization of the ratio A/E), stomata should function such that the marginal water cost of

carbon assimilation $(\frac{\partial A}{\partial E})$ remains constant (Cowan and Farquhar, 1977; Farquhar and Sharkey, 1982). This aspect of stomatal control couples the structural traits involved with water-flow with traits associated with primary production (Brodribb and Holbrook, 2007) and explains observed correlations between K_{leaf} and A_{max} in a number of studies (Brodribb et al., 2007; Brodribb et al., 2010; Brodribb et al., 2005; Brodribb and Jordan, 2008; Sack and Holbrook, 2006; Sack and Scoffoni, 2013). The length of hydraulic pathway is directly proportional to K_{leaf} (Brodribb et al., 2007) and the A/g_s ratio determines foliar $\Delta^{13}C$ (and WUE$_i$) signatures in leaves. Thus, the constraint on K_{leaf} by LVD affects the coordination between the processes of A and E and thereby might explain significant relationships between structural (LVD) and functional traits (WUE$_i$). For the two deep-rooted species, having access to groundwater resulted in convergence to a common solution for optimizing water supply through veins with respect to E (Brodribb and Holbrook, 2007).

Several robust and testable predictions arise from the conclusion that *E. camaldulensis* and *C. opaca* are functioning at a semi-arid site as though they have access to *ca* 1700 or 900 mm rainfall, respectively. Species growing in high rainfall zones possess a suite of traits, including low density sapwood, large diameter xylem vessels, small resistance to vessel implosion, large SLA and a large maximum stomatal conductance, compared to species growing in arid regions (O'Grady et al., 2006b; O'Grady et al., 2009; Wright et al., 2004). Therefore, these attributes should be present in *E. camaldulensis* and *C. opaca* if they are functioning as though they are growing in a mesic environment. We have previously established (Eamus et al., 2016; Santini et al., 2016) that these predictions are confirmed by field data and therefore conclude that analyses of foliar $\Delta^{13}C$ has global application to the preservation and understanding of GDEs.

4.3 Conclusions

We posed five questions regarding depth-to-groundwater (DTGW), foliar discrimination against ^{13}C ($\Delta^{13}C$) and leaf vein density (LVD) as underpinning the rationale for this study. We confirmed that access to shallow groundwater by *E. camaldulensis* and *C. opaca* (DTGW *ca* 0 –11 m) resulted in smaller WUE$_i$ than *A. aneura*. We also demonstrated that LVD correlated with DTGW for the shallower depths (< 10 m) in *E. camaldulensis* and *C. opaca*, but not in *A. aneura*. We further demonstrated that there was correlation between LVD and $\Delta^{13}C$ (and hence WUE$_i$) for *E. camaldulensis* and *C. opaca*, but not in *A. aneura*. Similarly, as distance increased from a creek near a flood-out associated with aquifer recharge, foliar $\Delta^{13}C$ decreased and WUE$_i$ increased for *E. camaldulensis* and *C. opaca*, but not for *A. aneura*. Finally, we conclude that foliar $\Delta^{13}C$ can be used as an indicator of utilisation of groundwater or stored soil water by vegetation in arid regions, providing an inexpensive and rapid alternative to the stable isotopes of water that have been used in many previous studies. The observation that the $\Delta^{13}C$ of the two groundwater-using species was distant from the continental regression of $\Delta^{13}C$ against rainfall (Fig. 8) is strong evidence of the value of $\Delta^{13}C$ as an indicator of utilisation of water that is additional to rainfall, and this supplemental water can be derived from either groundwater or soil recharge arising in flood-out zones of creeks.

5 Author contributions

All authors contributed to field data sampling. RR undertook all the isotope analyses and statistical analyses and wrote the thesis that formed the basis of this Ms. DE oversaw the design and implementation of the entire project. All authors contributed to writing this Ms and interpretation of the data.

6 Acknowledgements

7 References

Beer, C., Ciais, P., Reichstein, M., Baldocchi, D., Law, B.E., Papale, D., Soussana, J.F., Ammann, C., Buchmann, N., Frank, D., Gianelle, D., Janssens, I.A., Knohl, A., Kostner, B., Moors, E., Roupsard, O., Verbeeck, H., Vesala, T., Williams, C.A., Wohlfahrt, G.: Temporal and among-site variability of inherent water use efficiency at the ecosystem level, Glob. Biogeochem. Cycles 23 (GB2018), DOI: 10.1029/2008GB003233, 2009.

Benyon, R. G., Theiveyanathan, S., and Doody, T. M.: Impacts of tree plantations on groundwater in south-eastern Australia, Aus. J. of Bot., 54, 181–192, doi:10.1071/bt05046, 2006.

Box, J.B., Duguid, A., Read, R.E., Kimber, R.G., Knapton, A., Davis, J. and Bowland, A.E.: Central Australian waterbodies: The importance of permanence in a desert landscape. J. Arid Environ., 72, 1395-1413, DOI: 10.1016/j.jaridenv.2008.02.022, 2008.

Brodribb, T.J., Feild, T.S. and Jordan, G.J.: Leaf maximum photosynthetic rate and venation are linked by hydraulics, Pl. Phys., 144(4), 1890-1898, 2007.

Brodribb, T.J., Feild, T.S. and Sack, L.: Viewing leaf structure and evolution from a hydraulic perspective, Funct. Pl. Biol., 37(6), 488-498, 2010.

Brodribb, T.J. and Holbrook, N.M.: Changes in leaf hydraulic conductance during leaf shedding in seasonally dry tropical forest, New Phyt., 158(2), 295-303, 2003.

Brodribb, T.J. and Holbrook, N.M.: Forced depression of leaf hydraulic conductance in situ: effects on the leaf gas exchange of forest trees, Func. Ecol., 21(4), 705-712, 2007.

Brodribb, T.J., Holbrook, N.M., Zwieniecki, M.A. and Palma, B.: Leaf hydraulic capacity in ferns, conifers and angiosperms: impacts on photosynthetic maxima. New Phyt., 165(3), 839-846, 2005.

Brodribb, T.J. and Jordan, G.J.: Internal coordination between hydraulics and stomatal control in leaves, Pl. Cell & Environ., 31(11), 1557-1564, 2008.

Bucci, S., Goldstein, G., Meinzer, F., Scholz, F., Franco, A. and Bustamante, M.: Functional convergence in hydraulic architecture and water relations of tropical savanna trees: from leaf to whole plant, Tree Physiol., 24(8), 891-899, 2004.

Budyko, M.I.: Climate and Life. Academic Press, New York, 508 pp, 1974.

Byrne, M., Yeates, D.K., Joseph, L., Kearney, M., Bowler, J., Williams, M.A.J., Cooper, S., Donnellan, S.C., Keogh, J.S. and Leys, R.: Birth of a biome: insights into the assembly and maintenance of the Australian arid zone biota, Molec. Ecol., 17(20), 4398-4417, 2008.

Calf, G.E., McDonald, P.S. and Jacobson, G.: Recharge mechanism and groundwater age in the Ti-Tree basin, Northern Territory, Aus. J.of Earth Sci., 38: 299–306, DOI: 10.1080/08120099108727974, 1991.

Cernusak, L.A., Hutley, L.B., Beringer, J., Holtum, J.A. and Turner, B.L.: Photosynthetic physiology of eucalypts along a sub-continental rainfall gradient in northern Australia, Agri. and For. Met., 151(11), 1462-1470, 2011.

Clarke, R.: Water: the international crisis. Earthscan, London, UK, 1991.

Cleverly, J.: Alice Springs Mulga OzFlux site. TERN OzFlux: Australian and New Zealand Flux Research and Monitoring Network, hdl.handle.net/102.100.100/8697, 2011.

Cleverly, J.: Ti Tree East OzFlux Site. TERN OzFlux: Australian and New Zealand Flux Research and Monitoring Network, hdl.handle.net/102.100.100/11135, 2013.

Cleverly, J., Boulain, N., Villalobos-Vega, R., Grant, N., Faux, R., Wood, C., Cook, P.G., Yu, Q., Leigh, A. and Eamus, D.: Dynamics of component carbon fluxes in a semi-arid Acacia woodland, central Australia, J. Geophys. Res.,: Biogeosciences, 118(3), 1168-1185, 2013.

Cleverly, J., Eamus, D., Van Gorsel, E., Chen, C., Rumman, R., Luo, Q., Coupe, N.R., Li, L., Kljun, N. and Faux, R.: Productivity and evapotranspiration of two contrasting semiarid ecosystems following the 2011 global carbon land sink anomaly, Agric. and For. Met., 220, 151-159, 2016a.

Cleverly, J., Eamus, D., Restrepo Coupe, N., Chen, C., Maes, W., Li, L., Faux, R., Santini, N.S., Rumman, R., Yu, Q. and Huete, A.: Soil moisture controls on phenology and productivity in a semi-arid critical zone, Sci. of the Total Environ., 568, 1227-1237, DOI: 10.1016/j.scitotenv.2016.05.142, 2016b.

Cook, P.G., O'Grady, A.P., Wischusen, J.D.H., Duguid, A., Fass, T., Eamus, D. and Palmerston, N.T.: *Ecohydrology of sandplain woodlands in central Australia*. Department of Natural Resources, Environment and The Arts, Northern Territory Government, Darwin, 2008a.

Cook, P. G., Hatton, T. J., Pidsley, D., Herczeg, A. L., Held, A., O'Grady, A., and Eamus, D.: Water balance of a tropical woodland ecosystem, northern Australia: a combination of micro-meteorological, soil physical and groundwater chemical approaches, J. of Hyd. 210, 161–177, doi:10.1016/S0022-1694(98)00181-4, 2008b.

Cowan, I.R. and Farquhar, G.D.: Stomatal function in relation to leaf metabolism and environment. The Society for Experimental Biology Symposium pp. 471-505. 1997.

Craig, H.: Isotopic variations in meteoric waters. Science. 133: 1702-1703, 1961.

Cullen, L.E. and Grierson, P.F.: A stable oxygen, but not carbon, isotope chronology of *Callitris columellaris* reflects recent climate change in north-western Australia, Climatic Change. 85, 213-229, DOI: 10.1007/s10584-006-9206-3, 2007.

Donohue, R.J., McVicar, T. and Roderick, M.L.: Climate-related trends in Australian vegetation cover as inferred from satellite observations, 1981–2006, Glob. Change Biol., 15(4), 1025-1039, 2009.

Eamus, D., Cleverly, J., Boulain, N., Grant, N., Faux, R. and Villalobos-Vega, R.: Carbon and water fluxes in an arid-zone Acacia savanna woodland: An analyses of seasonal patterns and responses to rainfall events, Agric. and For. Met., 182, 225-238, 2013.

Eamus, D., Hatton, T., Cook, P. and Colvin, C.: *Ecohydrology: vegetation function, water and resource management*. CSIRO Publishing: Melbourne, 2006.

Eamus, D., O'Grady, A.P. and Hutley, L.: Dry season conditions determine wet season water use in the wet–tropical savannas of northern Australia, Tree Phys., 20(18), 1219-1226, 2000.

Eamus, D., Zolfaghar, S., Villalobos-Vega, R., Cleverly, J. and Huete, A.: Groundwater-dependent ecosystems: recent insights from satellite and field-based studies, Hyd. and Earth Sys. Sci., 19, 4229-4256, DOI: 10.5194/hess-19-4229-2015, 2015.

Eamus, D., Huete, A., Cleverly, J., Nolan, R.H., Ma, X., Tarin, T. and Santini, N.S.: Mulga, a major tropical dry open forest of Australia: recent insights to carbon and water fluxes, Env. Res. Lett., 11, 125011, DOI: 10.1088/1748-9326/11/12/125011, 2016.

Ehleringer J.R. and Cooper T.A.: Correlation between carbon isotope ratio and microhabitat in desert plants, Oecologia 76, 562 – 566, 1988.

Farquhar, G.D. and Sharkey, T.D.: Stomatal conductance and photosynthesis. Ann. Rev. of Pl. Phys., 33(1), 317-345, 1982.

Gardner, R.O.: An overview of botanical clearing technique. Stain Tech., 50(2), 99-105, 1975.

Grigg, A.M., Lambers, H. and Veneklaas, E.J.: Changes in water relations for *Acacia ancistrocarpa* on natural and mine-rehabilitation sites in response to an experimental wetting pulse in the Great Sandy Desert, Pl. and Soil, 326(1-2), 75-96, 2010.

Hacke, U.G., Sperry, J.S., Ewers, B.E., Ellsworth, D.S., Schäfer, K.V.R. and Oren, R.: Influence of soil porosity on water use in *Pinus taeda,* Oecologia, 124(4), 495-505, 2000.

Hernández, E., Pausas, J.G. and Vilagrosa, A.: Leaf physiological traits in relation to resprouter ability in the Mediterranean Basin, Pl. Ecol., 212(12), 1959-1966, 2011.

Howe, P., O'Grady, A.P., Cook, P.G. and Fas, T.: Project REM1 – A Framework for Assessing Environmental Water Requirements for Groundwater Dependent Ecosystems Report-2 Field Studies. Land and Water Australia, 2007.

Hutley, L.B., Beringer, J., Isaac, P.R., Hacker, J.M. and Cernusak, L.A.: A sub-continental scale living laboratory: Spatial patterns of savanna vegetation over a rainfall gradient in northern Australia, Agric. and For. Met. 151(11), 1417-1428, 2011.

IAEA,: Reference Sheet for VSMOW2 and SLAP2 international measurement standards. International Atomic Energy Agency, Vienna, 2009.

Ingraham, N.L. and Shadel, C.: A comparison of the toluene distillation and vacuum/heat methods for extracting soil water for stable isotopic analysis, J. of Hyd., 140(1), 371-387, 1992.

Karan, M., Liddell, M., Prober, S., Arndt, S., Beringer, J., Boer, M., Cleverly, J., Eamus, D., Grace, P., van Gorsel, E., Hero, J.-M., Hutley, L., Macfarlane, C., Metcalfe, D., Meyer, W., Pendall, E., Sebastian, A. and Wardlaw, T.: The Australian SuperSite Network: a continental, long-term terrestrial ecosystem observatory, Sci.of the Total Environ., 568, 1263–1274, DOI: 10.1016/j.scitotenv.2016.05.170, 2016.

Leffler, A.J. and Evans, A.S.: Variation in carbon isotope composition among years in the riparian tree *Populus fremontii,* Oecologia, 119(3), 311-319, 1999.

Maslin, B.R. and Reid, J.E.: A taxonomic revision of Mulga (*Acacia aneura* and its close relatives: Fabaceae) in Western Australia, Nuytsia, 22, 129–167, 2012.

Medlyn, B.E., Duursma, R.A., Eamus, D., Ellsworth, D.S., Prentice, I.C., Barton, C.V.M., Crous, K.Y., De Angelis, P., Freeman, M. and Wingate, L.: Reconciling the optical and empirical approaches to modelling stomatal conductance, Glob. Change Biol., 17, 2134-2144, 2011.

Meinzer, F.C. and Grantz, D.A.: Stomatal and hydraulic conductance in growing sugarcane: stomatal adjustment to water transport capacity, Pl., Cell and Environ., 13(4), 383-388, 1990.

Miller, J.M., Williams, R.J. and Farquhar, G.D.: Carbon isotope discrimination by a sequence of *Eucalyptus* species along a subcontinental rainfall gradient in Australia, Func. Ecol., 15(2), 222-232, 2001.

Morton, S., Smith, D.S., Dickman, C.R., Dunkerley, D., Friedel, M., McAllister, R., Reid, J., Roshier, D., Smith, M. and Walsh, F.: A fresh framework for the ecology of arid Australia, J. of Arid Envir., 75(4), 313-329, 2011.

Niinemets, Ü., Portsmuth, A., Tena, D., Tobias, M., Matesanz, S. and Valladares, F.: Do we underestimate the importance of leaf size in plant economics? Disproportional scaling of support costs within the spectrum of leaf physiognomy, Annals of Bot., 100(2), 283-303, 2007.

Niinemets, Ü., Portsmuth, A. and Tobias, M.: Leaf size modifies support biomass distribution among stems, petioles and mid-ribs in temperate plants, New Phyt., 171(1), 91-104, 2006.

Niklas, K.J., Cobb, E.D., Niinemets, Ü., Reich, P.B., Sellin, A., Shipley, B. and Wright, I.J.: "Diminishing returns" in the scaling of functional leaf traits across and within species groups, Proceedings of the National Academy of Sciences, 104(21): 8891-8896, 2007.

Nolan, R.H., Fairweather, K.A., Tarin, T., Santini, N.S., Cleverly, J., Faux, R. and Eamus, D.: Divergence in plant water-use strategies in semiarid woody species, Func. Pl. Biol. In Press, DOI: 10.1071/FP17079, 2017.

NRETA,: The Ti Tree Basin Aquifer. Department of Natural Resources, Environment and the Arts, Water Resources Branch, Land and Water Division, https://supersites.tern.org.au/images/resource/TiTree_Basin_Groundwater.pdf, 2007.

NRETAS,: Ti Tree Basin Water Resource Report. Department of Natural Resources, Environment, the Arts and Sport, Natural Resource Management Division, Water Management Branch Document No. 04/2009A ISBN: 978-1-921519-21-5, 2009.

O'Grady, A.P., Carter, J.L. and Bruce, J.: Can we predict groundwater discharge from terrestrial ecosystems using existing eco-hydrological concepts? Hyd. and Earth Sys. Sci., 15(12), 3731-3739, 2011.

O'Grady, A.P., Cook, P.G., Eamus, D., Duguid, A., Wischusen, J.D.H., Fass, T. and Worldege, D.: Convergence of tree water use within an arid-zone woodland, Oecologia, 160(4): 643-655, 2009.

O'Grady, A.P., Cook, P.G., Howe, P. and Werren, G.: Groundwater use by dominant tree species in tropical remnant vegetation communities, Aus. J. of Bot., 54, 155-171, 2006a.

O'Grady, A.P., Eamus, D., Cook, P.G. and Lamontagne, S.: Comparative water use by the riparian trees *Melaleuca argentea* and *Corymbia bella* in the wet–dry tropics of northern Australia, Tree Phys., 26(2), 219-228, 2006b.

O'Grady, A.P., Eamus, D., Cook, P.G. and Lamontagne, S.: Groundwater use by riparian vegetation in the wet–dry tropics of northern Australia, Aus. J. of Bot., 54(2), 145-154.

O'Grady, A.P. and Holland, K., 2010. *Review of Australian groundwater discharge studies of terrestrial systems*. CSIRO National Water Commission, 2006c.

Pressland, A.J.: Productivity and management of mulga in south-western Queensland in relation to tree structure and density, Aus. J. of Bot., 23(6), 965-976, 1975.

Prior, L.D., Eamus, D. and Duff, G.A.: Seasonal and diurnal patterns of carbon assimilation, stomatal conductance and leaf water potential in *Eucalyptus tetrodonta* saplings in a wet–dry savanna in northern Australia, Aus. J. of Bot., 45(2), 241-258, 1997.

Reynolds, J.F., Smith, D.M.S., Lambin, E.F., Turner, B., Mortimore, M., Batterbury, S.P., Downing, T.E., Dowlatabadi, H., Fernández, R.J. and Herrick, J.E.: Global desertification: building a science for dryland development, Science, 316(5826): 847-851, 2007.

Rumman, R., Atkin O.K., Bloomfield K.J., and Eamus D.: Variation in bulk-leaf 13C discrimination, leaf traits and water use efficiency –trait relationships along a continental-scale climate gradient in Australia. Glob. Chng. Biol., 24, 1186-1200, 2017.

Sack, L., Cowan, P., Jaikumar, N. and Holbrook, N.: The 'hydrology'of leaves: co-ordination of structure and function in temperate woody species, Plant, Cell & Environment, 26(8): 1343-1356, 2003.

Sack, L. and Frole, K.: Leaf structural diversity is related to hydraulic capacity in tropical rain forest trees, Ecology, 87(2): 483-491, 2006.

Sack, L. and Holbrook, N.M.: Leaf hydraulics, Ann. Rev. of Pl. Biol., 57, 361-381, 2006.

Sack, L. and Scoffoni, C.: Leaf venation: structure, function, development, evolution, ecology and applications in the past, present and future, New Phyt., 198(4), 983-1000, 2013.

Santini, N.S., Cleverly, J., Faux, R., Lestrange, C., Rumman, R. and Eamus, D.: Xylem traits and water-use efficiency of woody species co-occurring in the Ti Tree Basin arid zone, Trees, 30(1), 295-303, 2016.

Schmidt, S., Lamble, R.E., Fensham, R.J. and Siddique, I.: Effect of woody vegetation clearing on nutrient and carbon relations of semi-arid dystrophic savanna, Pl. and Soil, 331(1-2), 79-90, 2010.

Scoffoni, C., Rawls, M., McKown, A., Cochard, H. and Sack, L.: Decline of leaf hydraulic conductance with dehydration: relationship to leaf size and venation architecture, Pl. Phys., 156(2), 832-843, 2011.

Shanafield, M., Cook, P.G., Gutiérrez-Jurado, H.A., Faux, R., Cleverly, J. and Eamus, D.: Field comparison of methods for estimating groundwater discharge by evaporation and evapotranspiration in an arid-zone playa, J. of Hyd., 527, 1073-1083, DOI: 10.1016/j.jhydrol.2015.06.003, 2015.

Singer, M. B., Sargean, C.I., Piegay, H., Riquier, J., Wilson, R.J.S., and Evans, C.N.: Floodplain ecohydrology: Climatic, anthropogenic, and local physical controls on partitioning of water sources to riparian trees, Water Resour. Res., 50, 4490–4513, 2014.

Sommerville, K.E., Gimeno, T.E. and Ball, M.C.: Primary nerve (vein) density influences spatial heterogeneity of photosynthetic response to drought in two *Acacia* species, Func. Pl. Biol., 37(9), 840-848, 2010.

Sommerville, K.E., Sack, L. and Ball, M.C.: Hydraulic conductance of *Acacia* phyllodes (foliage) is driven by primary nerve (vein) conductance and density. Pl. Cell and Environ., 35(1), 158-168, 2012.

Sperry, J.S.: Hydraulic constraints on plant gas exchange. Agric. and For. Met., 104(1), 13-23, 2000.

Stewart, G.R., Turnbull, M., Schmidt, S. and Erskine, P.: ^{13}C natural abundance in plant communities along a rainfall gradient: a biological integrator of water availability, Func. Pl. Biol., 22(1) 51-55, 1995.

Taylor, D.: Tree, leaf and branch trait coordination along an aridity gradient. PhD Thesis. University of Technology Sydney, 2008.

Thomas, D.S. and Eamus, D.: The influence of predawn leaf water potential on stomatal responses to atmospheric water content at constant C_i and on stem hydraulic conductance and foliar ABA concentrations, J. of Exp. Bot., 50(331), 243-251, 1999.

Thorburn, P.J., Mensforth, L.J. and Walker, G.R.: Reliance of creek-side river red gums on creek water, Mar. and Freshwater Res., 45(8), 1439-1443, 1994.

Uhl, D. and Mosbrugger, V.: Leaf venation density as a climate and environmental proxy: a critical review and new data, Palaeogeog., Palaeoclim., Palaeoecol., 149(1), 15-26, 1999.

Villeneuve, S., Cook, P.G., Shanafield, M., Wood, C. and White, N.: Groundwater recharge via infiltration through an ephemeral riverbed, central Australia, J.of Arid Envir., 117, 47-58, DOI: 10.1016/j.jaridenv.2015.02.009, 2015.

Warren, C.R., Tausz, M. and Adams, M.A.: Does rainfall explain variation in leaf morphology and physiology among populations of red ironbark (*Eucalyptus sideroxylon* subsp. *tricarpa*) grown in a common garden? Tree Phys., 25(11), 1369-1378, 2005.

Werner, C., Schnyder, H., Cuntz, M., Keitel, C., Zeeman, M., Dawson, T., Badeck, F.-W., Brugnoli, E., Ghashghaie, J. and Grams, T.: Progress and challenges in using stable isotopes to trace plant carbon and water relations across scales, Biogeosciences, 9, 3083-3111, 2012.

West, A.G., Patrickson, S.J. and Ehleringer, J.R.: Water extraction times for plant and soil materials used in stable isotope analysis, Rapid Comms. in Mass Spec., 20(8), 1317-1321, 2006.

Wright, I.J., Groom, P.K., Lamont, B.B., Poot, P., Prior, L.D., Reich, P.B., Schulze, E.D., Veneklaas, E.J. and Westoby, M.: Leaf trait relationships in Australian plant species, Func. Pl. Biol., 31, 551-558, DOI: 10.1071/fp03212, 2004.

Wright, B.R., Latz, P.K. and Zuur, A.F.: Fire severity mediates seedling recruitment patterns in slender mulga (*Acacia aptaneura*), a fire-sensitive Australian desert shrub with heat-stimulated germination, Pl. Ecol., 217, 789-800, DOI: 10.1007/s11258-015-0550-0, 2016.

Zolfaghar, S., Villalobos-Vega, R., Cleverly, J., Zeppel, M., Rumman, R. and Eamus, D.: The influence of depth-to-groundwater on structure and productivity of *Eucalyptus* woodlands, Aus. J. of Bot., 62(5), 428-437, 2014.

Zolfaghar, S., Villalobos-Vega, R., Cleverly, J. and Eamus, D.: Co-ordination among leaf water relations and xylem vulnerability to embolism of Eucalyptus trees growing along a depth-to-groundwater gradient, Tree Phys., 35, 732–743, DOI: 10.1093/treephys/tpv039, 2015.

Zolfaghar, S., Villalobos-Vega, R., Zeppel, M., Cleverly, J., Rumman, R., Hingee, M., Boulain, N., Li, Z., Eamus, D. and Tognetti, R.: Transpiration of *Eucalyptus* woodlands across a natural gradient of depth-to-groundwater, Tree Phys., 37, 961–975, DOI: 10.1093/treephys/tpx024, 2017.

**Table 1:** **A summary of plots, transects and spot measurements undertaken in the present study.**

| Plot/Transect Number		Species sampled	Replication	Isotopes analysed
Plots 1 - 4	4.4 - 13.9	*Eucalyptus camaldulensis, Acacia aneura (Mulga), Corymbia opaca*	2 or 3 trees per species, 3 - 5 samples per tree per isotope	^{18}O, deuterium of groundwater and xylem water; and ^{13}C of leaves/phyllodes
Transects 1 – 3 (Allungra Creek study)	Regional aquifer > 40 m but shallow ephemeral GW present after flood-outs	*Eucalyptus camaldulensis Acacia aneura*	2 or 3 trees per species, 3 or more samples per tree	^{13}C of leaves/ phyllodes
Additional spot measurements across the basin	20, 36 and 49.5	*Acacia aneura Corymbia opaca*	2 or 3 trees per species, 3 or more samples per tree	^{13}C of leaves/phyllodes

18

5

10

Figures

15
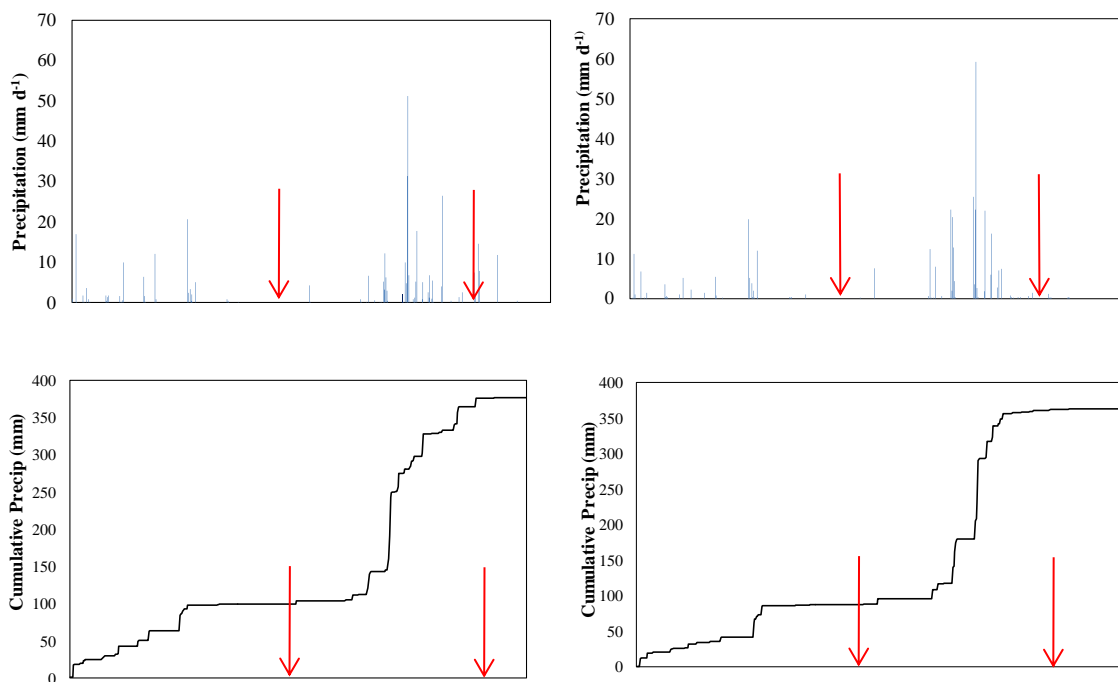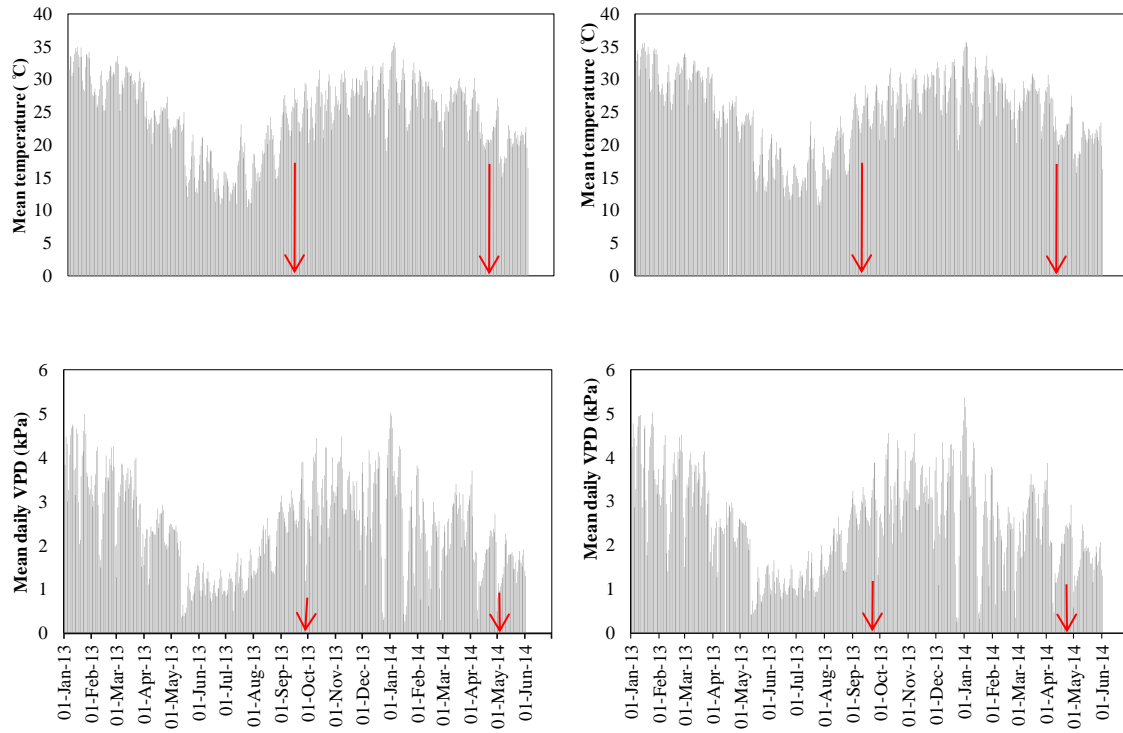
Figure 1:   Mean daily meteorological conditions of daily precipitation, cumulative precipitation, mean air temperature and vapour pressure deficit Jan 2013 - Jun 2014. Red lines show sampling periods in September 2013 (late dry-season) and April 2014 (late wet-season). Left panels show data from the western EC tower (DTGW 49.4 m), and right panels show data for the eastern EC tower (DTGW 8.8 m).
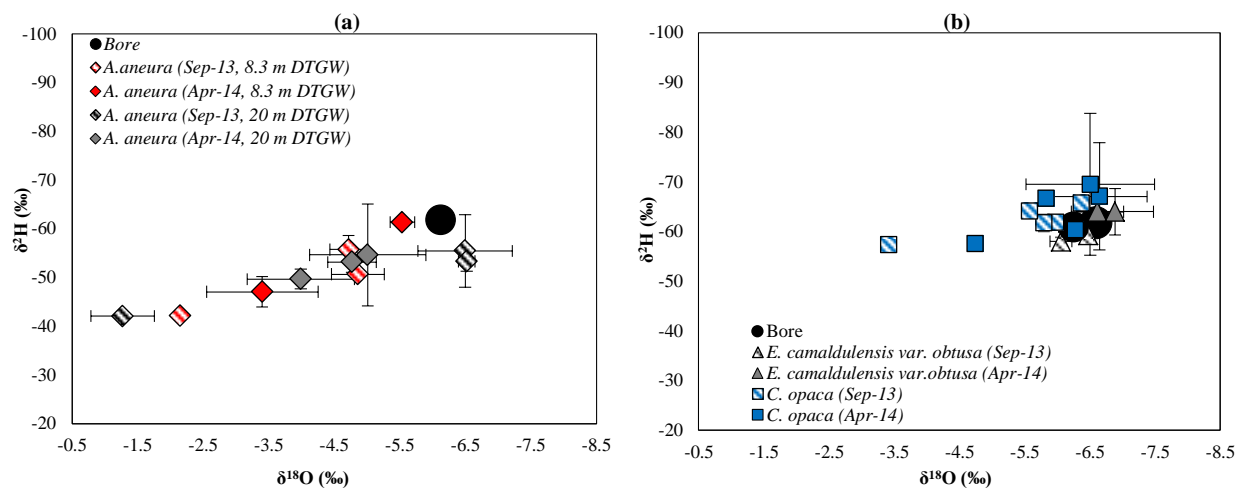
Figure 2: Comparison of xylem and bore water δ²H-δ¹⁸O plots for *Acacia aneura* sampled from 8.3 m and 20 m DTGW (a) and *Eucalyptus camaldulensis* and *Corymbia opaca* sampled from 4.4 m, 8.8 m and 13.9 m DTGW (b). Error bars represent ± one standard error.

5

10

15

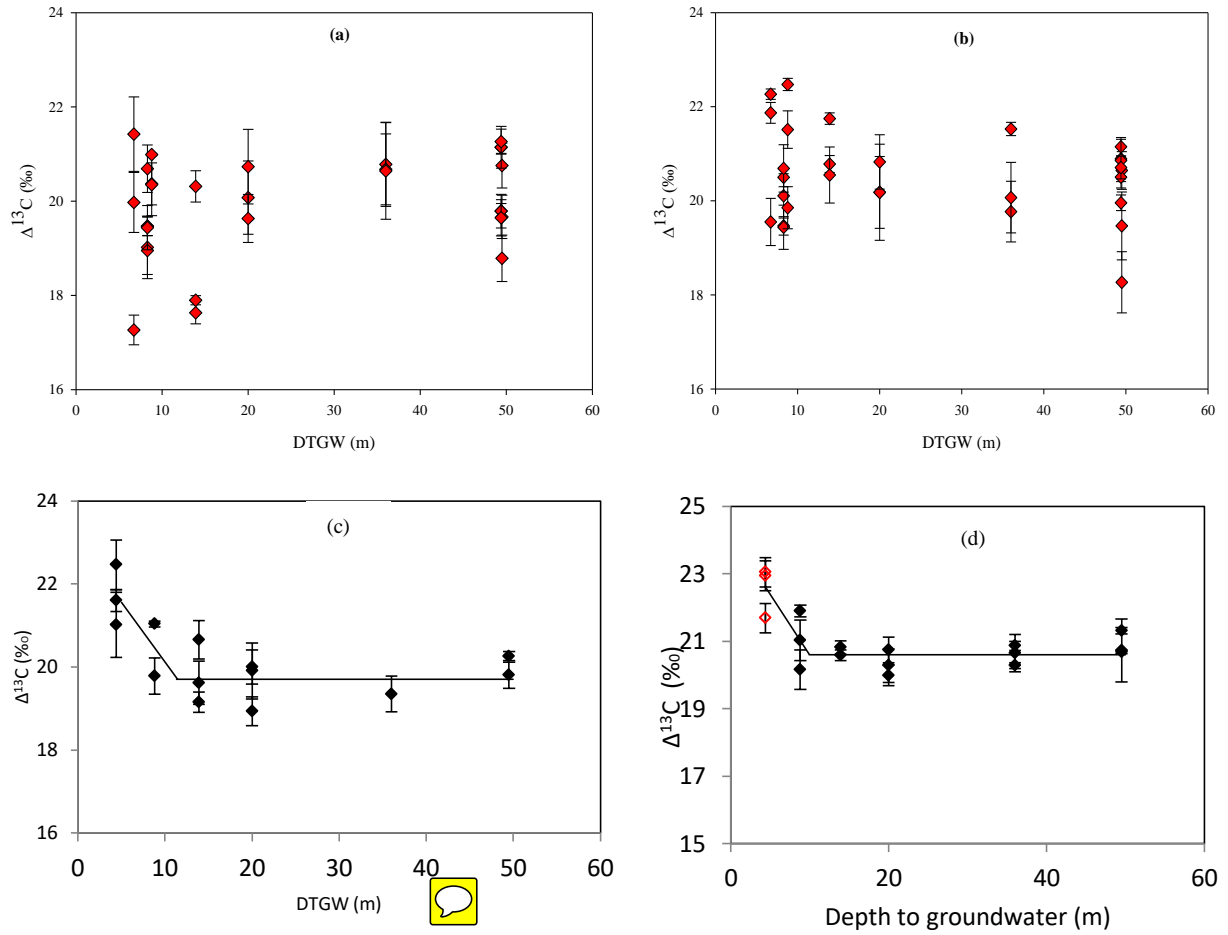**Sep-2013**   **Apr-2014**

Figure 3: Carbon isotope discrimination in leaf dry matter ($\Delta^{13}C$) plotted as a function of depth-to-groundwater (DTGW) in the Ti Tree basin. Panels (a) and (b) are data for *A. aneura* only; in panels (c) and (d) *C. opaca* (black symbols) and *E. camaldulensis* (red symbols) are presented. Left and right panels show Sep-2013 and Apr-2014 sampling respectively. Lines in panels (c) and (d) are from segmented regression of the combined data. Error bars represent ± one standard error.

5

(a)

(b)
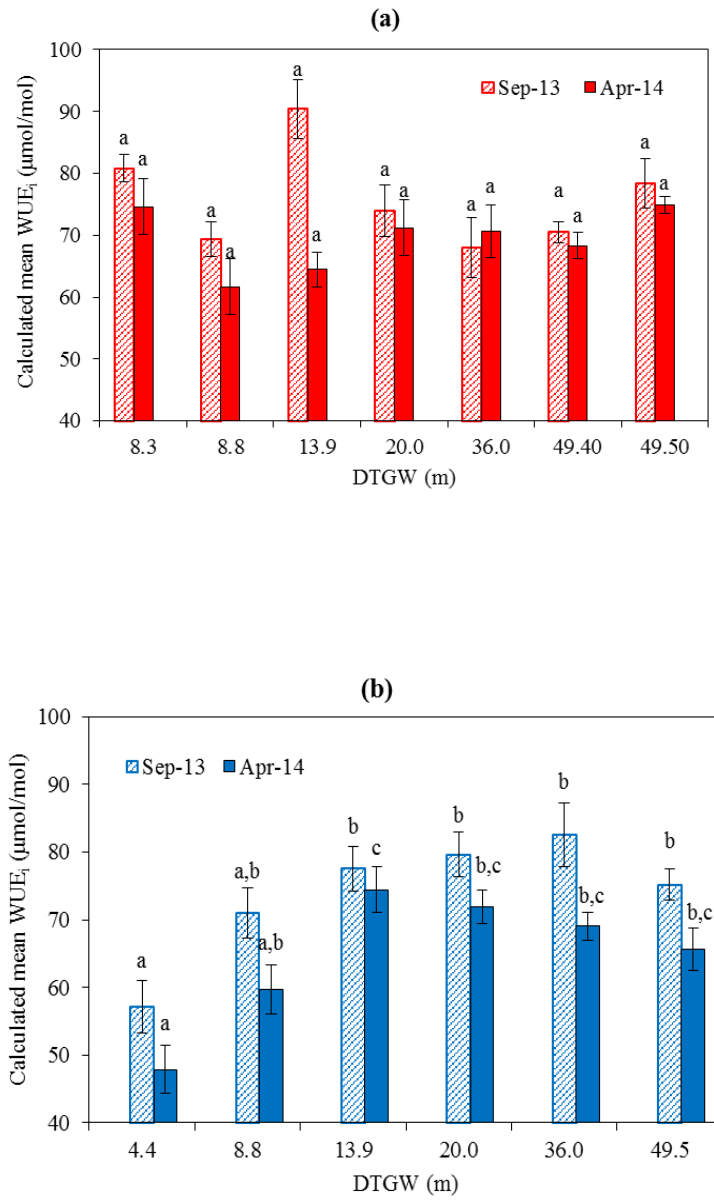
Figure 4: Leaf intrinsic water-use-efficiency (WUE_i) calculated from $\Delta^{13}C$ in shallow-rooted *A. aneura* (a) and deep-rooted *E. camaldulensis* and *C. opaca* (b) across study sites for Sep-2013 (patterned column) and Apr-2014 (filled column). Bars within a season with the same letter are not significantly different across the depth-to-groundwater gradient (Tukey HSD, p < 0.05). Error bars represent ± one standard error.

5

(a)

Δ¹³C (‰)

y = -0.422ln(x) + 21.616
R² = 0.9862

Distance from creek (m)

(b)

WUE$_i$ (µmol mol^{-1})

y = 4.5531ln(x) + 58.068
R² = 0.9862

Distance from creek (m)
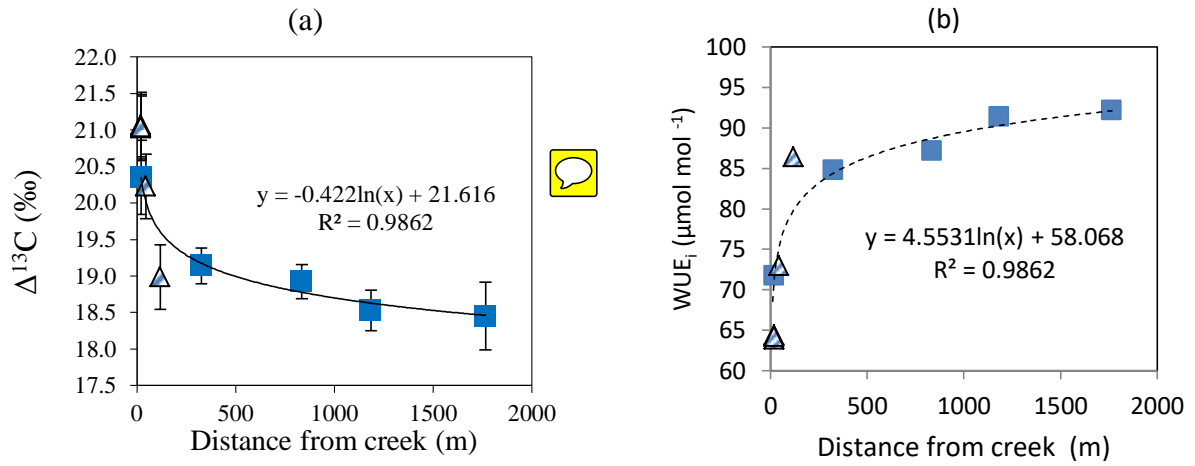
Figure 5:   Δ¹³C (a) and WUE$_i$ (b) of deep-rooted species sampled across Ti Tree basin plotted as functions of distance from Allungra Creek bed. Striped triangles represent *E. camaldulensis* and blue squares represent *C. opaca*. Error bars represent ± one standard error. The regression is fitted only to the *E. camuldulensis* data. Note that the largest value of Δ¹³C and the lowest value of WUE for *C. opaca* are three overlapping samples.
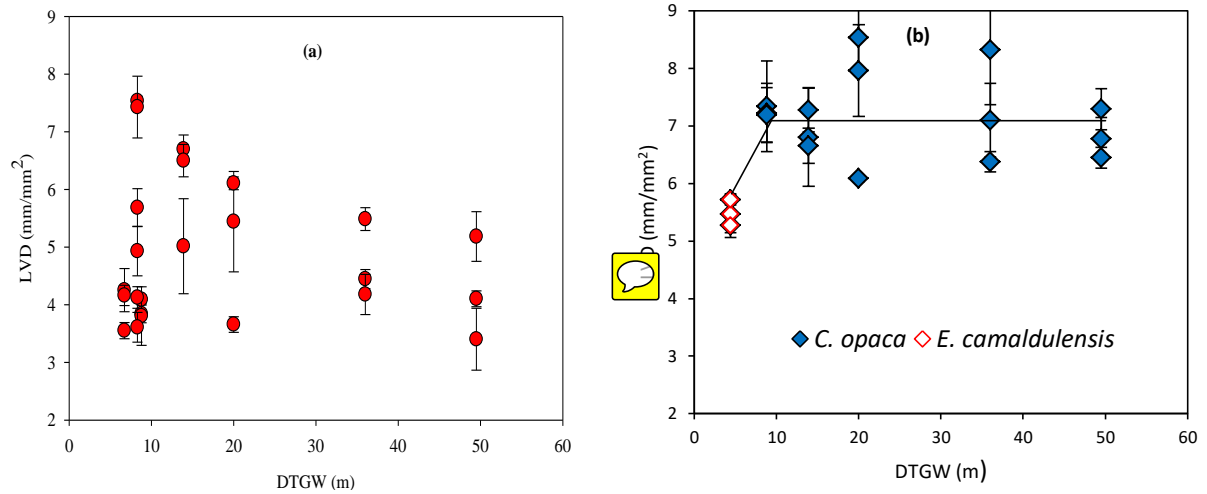
Figure 6:   Leaf vein density (LVD) of *A. aneura* (panel a) or *E. camaldulensis* (red symbols) and *C. opaca* (blue symbols) (panel b) as a function of depth-to-groundwater. Each symbol represents mean LVD calculated from three individual leaves. Error bars represent ± one standard error. A statistically significant correlation derived from segmented linear regression of leaf vein density, for *E. camaldulensis* and *C. opaca* data combined, with depth-to-groundwater (DTGW) is shown in panel (b). The r^2 and standard deviation slope of the regression below the break point in (b) are 0.976 a d 0.0031 respectively.

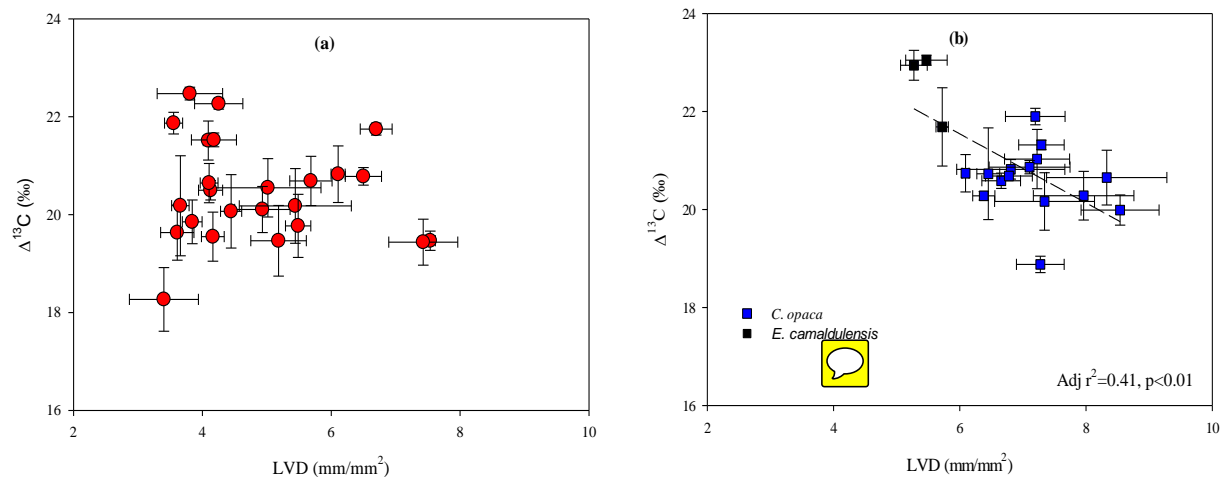Figure 7: Relationships of leaf vein density of (a) *A. aneura* and (b) *E. camaldulensis* (black symbols) and *C. opaca* (blue symbols) with bulk-leaf Δ¹³C. Each symbol represents mean LVD and Δ¹³C, with both variables measured on the same leaf. Error bars represent ± one standard error. A statistically significant correlation of LVD and Δ¹³C of *E. camaldulensis* and *C. opaca* is plotted with a dashed line.
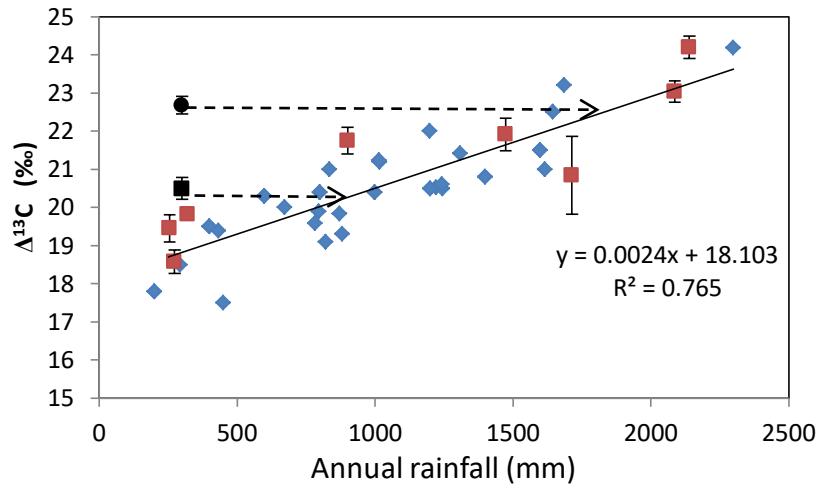
Figure 8:   Relationships of discrimination against carbon-13 ($\Delta^{13}C$) with annual rainfall observed in different studies across Australia. The diamonds represent observations made in eastern Australia (Stewart et al., 1995), northern Australia (Miller et al., 2001) and sites in New South Wales (Taylor, 2008). The red squares are data from a continental-scale assessment of foliar $\Delta^{13}C$ (Rumman et al., 2017). The black circle is the mean $\Delta^{13}C$ of *E. camaldulensis* and the black square is the mean $\Delta^{13}C$ *C. opaca*, both of which were measured in the current study. The 95 % CI for the mean $\Delta^{13}C$ is $\pm$ 0.403 and the s.e of the slope is 0.000231. The black dashed arrows indicate the rainfall that would be required to account for the $\Delta^{13}C$ for *E. camaldulensis* and *C. opaca* if these two species relied only upon rainfall.

Supplementary Material

Table S1: List of species, their functional types, $\Delta^{13}C$ and calculated intrinsic WUE$_i$ (plant functional type codes: BlT= broad leaf tree, NlT= needle leaf tree and S=shrub).

Species	Site	PFT	$\Delta^{13}C$ (‰)	Calculated WUE$_i$
Acacia aneura	AMU	NlT	19.71±0.21	78.67
Acacia melanoxylon	WR	BlT	22.46±0.46	49.00
Acmena graveolens	CT	BlT	21.96±0.31	54.37
Alphitonia whitei	RC	BlT	24.81±0.58	23.63
Alstonia muelleriana	RC	BlT	23.42±0.4	38.58
Alstonia scholaris	CT	BlT	22.76±0.36	45.75
Anopterus glandulosus	WR	S	25.58±0.44	15.34
Argyrodendron peralatum	CT	BlT	24.89±0.26	22.75
Atherosperma moschatum	WR	BlT	22.57±0.85	47.80
Cardwellia sublimis	CT	BlT	22.46±0.58	48.92
Castanospermum australe	CT	BlT	22.04±0.4	53.48
Ceratopetalum succirubrum	RC	BlT	26.52±0.13	5.21
Corymbia terminalis	AMU	BlT	19.89±0.29	76.65
Cryptocarya mackinnoniana	CT	BlT	24.59±0.12	26.02
Daphnandra repandula	RC	BlT	23.69±0.57	35.69
Doryphora aromatica	RC	BlT	25.41±0.88	17.19
Dysoxylum papuanum	CT	BlT	20.83±0.44	66.59
Elaeocarpus grandis	CT	BlT	22.34±0.1	50.30
Endiandra leptodendron	CT	BlT	26.86±0.6	1.51
Eucalyptus amplifolia	CP	BlT	21.02±0.31	64.53
Eucalyptus camaldulensis	AMU	BlT	20.28±0.35	72.43
Eucalyptus clelandii	GWW	BlT	17.68±0.17	100.56
Eucalyptus dumosa	CM	BlT	19.01±0.42	86.15
Eucalyptus fibrosa	CP	BlT	23.24±0.32	40.57

Species	Site	PFT	$\Delta^{13}C$ (‰)	Calculated WUE$_i$
Eucalyptus miniata	LF	BlT	21.86±0.07	55.39
Eucalyptus moluccana	CP	BlT	21.48±0.24	59.50
Eucalyptus obliqua	WR	BlT	22.01±0.73	53.79
Eucalyptus salmonophloia	GWW	BlT	18.88±0.09	87.56
Eucalyptus salubris	GWW	BlT	18.02±0.19	96.82
Eucalyptus socialis	CM	BlT	19.94±0.18	76.17
Eucalyptus tereticornis	CP	BlT	21.27±0.26	61.85
Eucalyptus tetrodonta	LF	BlT	19.82±0.34	77.39
Eucalyptus transcontinentalis	GWW	BlT	19.75±0.31	78.24
Eucryphia lucida	WR	BlT	22.07±0.06	53.16
Ficus leptoclada	RC	BlT	21.53±0.49	59.01
Ficus variegata	CT	BlT	21.85±0.29	55.60
Flindersia bourjotiana	RC	BlT	23.8±0.43	34.54
Gillbeea adenopetala	RC	BlT	24.41±0.26	27.94
Gillbeea whypallana	CT	BlT	23.22±0.42	40.79
Leptospermum lanigerum	WR	BlT	21.61±0.39	58.15
Litsea leefeana	RC	BlT	23.9±0.48	33.38
Melaleuca squarrosa	WR	BlT	21.94±0.25	54.60
Myristica globosa	CT	BlT	24.04±0.53	31.91
Notelaea ligustrina	WR	BlT	21.2±0.51	62.52
Nothofagus cunninghamii	WR	BlT	21.06±0.59	64.02
Phyllocladus aspleniifolius	WR	S	18.48±0.68	91.93
Pittosporum bicolor	WR	BlT	19.99±0.67	75.63
Polyscias elegans	RC	BlT	22.96±0.6	43.60
Pomaderris apetala	WR	S	23.55±0.44	37.21
Prunus turneriana	RC	BlT	25.83±0.74	12.59
Rockinghamia angustifolia	CT	BlT	22.69±0.35	46.49
Synima cordierorum	CT	BlT	22.8±0.39	45.33
Syzygium johnsonii	RC	BlT	25.7±0.07	13.99

Species	Site	PFT	$\Delta^{13}C$ (‰)	Calculated WUE$_i$
Syzygium sayeri	CT	BlT	23.01±0.46	43.04
Tasmannia lanceolata	WR	S	21.8±0.26	56.03
Xanthophyllum octandrum	CT	BlT	22.64±0.6	47.08

6
7

8   **Table S2: List of climate variables used in climate analysis**

WorldClim Code	Variables
BIO_1	Mean Annual Temperature
BIO_2	Mean Diurnal Range
BIO_3	Isothermality
BIO_4	Temperature Seasonality
BIO_5	Max Temperature of Warmest Month
BIO_6	Min Temperature of Coldest Month
BIO_7	Temperature Annual Range
BIO_8	Mean Temperature of Wettest Quarter
BIO_9	Mean Temperature of Driest Quarter
BIO_{10}	Mean Temperature of Warmest Quarter
BIO_{11}	Mean Temperature of Coldest Quarter
BIO_{12}	Mean Annual Precipitation
BIO_{13}	Precipitation of Wettest Month
BIO_{14}	Precipitation of Driest Month
BIO_{15}	Precipitation Seasonality
BIO_{16}	Precipitation of Wettest Quarter
BIO_{17}	Precipitation of Driest Quarter
BIO_{18}	Precipitation of Warmest Quarter
BIO_{19}	Precipitation of Coldest Quarter

9

10

11

12

13

14

15

Table S3: **Relationships of leaf traits with Mean Annual Precipitation and Moisture Index**

Traits	Correlated with ln MAP						Correlated with MI					
	Dry-season			Wet-season			Dry-season			Wet-season		
	Adj r²	*slope*	*p*	*Adj r²*	*slope*	*p*	*Adj r²*	*slope*	*p*	*Adj r²*	*slope*	*p*
A_{400}	**0.224**	+	<0.0001	NS		> 0.05	**0.071**	+	< 0.05	NS		> 0.05
Ln E_{400}	**0.140**	+	<0.001	**0.142**	+	< 0.01	0.04	+	> 0.05	NS		> 0.05
Ln $vpdL_{400}$	**0.281**	-	<0.0001	NS		> 0.05	**0.119**	-	<0.0001	NS		> 0.05
sqrt g_{s400}	**0.414**	+	<0.0001	**0.119**	+	< 0.01	**0.142**	+	<0.01	NS		> 0.05
Ln WUE_i	**0.481**	-	<0.0001	**0.420**	-	<0.0001	**0.206**	-	<0.0001	**0.357**	-	<0.0001
C_i/C_a	**0.332**	+	<0.0001	**0.337**	+	<0.0001	**0.192**	+	<0.0001	**0.380**	+	<0.0001
C_{i400}	**0.352**	+	<0.0001	**0.439**	+	<0.0001	**0.199**	+	<0.0001	**0.443**	+	<0.0001
LDMC	**0.349**	-	<0.0001	**0.331**	-	<0.0001	**0.277**	-	<0.0001	**0.366**	-	<0.0001
Ln LMA	**0.569**	-	<0.0001	**0.534**	-	<0.0001	**0.412**	-	<0.0001	**0.504**	-	<0.0001
Ln FMA	**0.532**	-	<0.0001	**0.516**	-	<0.0001	**0.369**	-	<0.0001	**0.452**	-	<0.0001
Ln Leaf N_{mass}	**0.192**	+	<0.001	**0.264**	+	<0.001	NS		> 0.05	**0.302**	+	<0.0001
Ln Leaf P_{mass}	**0.259**	+	<0.0001	NS		> 0.05	NS		> 0.05	NS		> 0.05
Ln Ratio N/P	**0.102**	-	<0.01	**0.167**	+	< 0.01	NS		> 0.05	**0.09**	+	< 0.05
Ln Leaf N_{area}	**0.178**	-	<0.0001	**0.269**	-	<0.001	**0.363**	-	<0.0001	**0.204**	-	<0.01
Ln Leaf P_{area}	N/S		> 0.05	**0.399**	-	<0.0001	**0.228**	-	<0.001	**0.286**	-	<0.0001
$A_{400}.N$	**0.403**	+	<0.0001	**0.162**	+	<0.01	**0.396**	+	<0.0001	NS		> 0.05
Ln $A_{400}.P$	**0.106**	+	< 0.01	**0.272**	+	<0.001	**0.334**	+	<0.001	**0.119**	+	<0.01

17 NS = Non-significant
18
19
20
21
22
23 **Table S4:** **Variation in $\Delta^{13}C$ and WUE_i by biome.**
24 Mean and s.e of wet and dry season $\Delta^{13}C$ and WUE_i. Means followed by different letters across sites in each
25 season are significantly different (Tukey HSD, confidence level of 0.05).

26

Site	$\Delta^{13}C$ (‰)		WUE_i (‰)	
	Dry-season	Wet-season	Dry-season	Wet-season
SW	19.75±0.49c	19.15±0.32a	78.14±5.26a	84.60±4.30a
STS	19.82±0.25c	20.15±0.40a	77.35±2.74a	73.85±3.45a
TW	20.16±0.25c	20.18±0.28a	73.84±4.10a	73.57±3.03a
HTS	20.77±0.38b,c	-	67.21±2.84a,b	-
TWF	21.54±0.55b,c	23.51±0.56b	68.80±5.91a,b	37.68±6.12a,b
LTR	22.98±0.46a,b	23.02±0.39b	43.25±4.93a,b	42.86±4.17a,b
UTR	24.05±0.76a	24.31±0.52b	31.74±8.16a	29.04±5.62b

27

28

29

30   **Brief site descriptions** of the seven Supersites **(8 nodes)**

31   **Calperum Mallee**

32   The Calperum Mallee SuperSite is in the mallee semi-arid ecosystem located approximately 25 km

33   north of Renmark in South Australia. The landscape is an extensive plain with undulating mallee

34   woodland and riverine vegetation that fringes the River Murray and its anabranches. The vegetation

35   is dominated by upper storey Eucalypt trees of four species (*Eucalyptus dumosa, Eucalyptus*

36   *incrassata, Eucalyptus oleosa* and *Eucalyptus socialis*) (Meyer *et al.*, 2015).

37   **Great Western Woodlands**

38   The Great Western Woodlands located in south-west Western Australia is the largest remaining

39   intact semi-arid temperate woodland in the world. The vegetation comprises a 16-million hectare

40   mosaic of mallee, scrub–heath and woodland and is locally determined by edaphic factors and

41   influenced by historic disturbances (Gosper *et al.*, 2013). Mean annual rainfall is ~250 mm with the

42   highest-mean rainfall months in winter. *Eucalyptus salubris* constructs the dominant crown layer in

43   association with other *Eucalyptus* species (*E. salmonophloia, E. longicornis and E. moderata)* (Gosper

44   *et al.*, 2013).

45   **Alice Mulga**

46   The semi-arid Alice Mulga SuperSite is located approximately 200 km north of Alice Springs, in the

47   Northern Territory of Australia. The climate is characterized as having hot summers and warm

48   winters. Mean annual rainfall is ~300 mm and is highly seasonal, mostly occurring in large rainfall

49   events during summer. Vegetation is dominated by Mulga (*Acacia aneura* and related species)

50   woodlands, occasionally with large areas of spinifex under sparse woodland of *Corymbia* and other

51   *Acacia* species (Cleverly et al., 2016).

52   **Cumberland Plain**

53   The Cumberland Plain is a sclerophyll *Eucalyptus* woodland west of Richmond in New South Wales.

54   The soil is characterized by nutrient-poor alluvium from sandstone and shale bedrock in the Blue

55   Mountains deposited by the Nepean River. Despite being nutrient poor, this SuperSite supports high

56   regional biodiversity and endemic biota and is dominated by *Eucalyptus fibrosa*, *E. moluccana* and *E.*

57   *tereticornis* in the overstorey. Mean annual precipitation of this site is 900 mm (Table 1).

58   **Warra Tall Eucalypt**

59   The Warra Tall Eucalypt SuperSite is a cool, wet temperate forest located in Tasmania. Vegetation is

60   dominated by tall *Eucalyptus obliqua* occurring in a full range of successional stages from young

61   regrowth forests to old-growth mixed forests (Hickey *et al.*, 1999). Mean annual temperature at this

62   site is the lowest (~10°C), with a mean annual precipitation of 1474 mm (Table 1).

63   **Litchfield Savanna**

64   The Litchfield Savanna SuperSite is a ~1.5 km^2 tropical savanna 70 km south of Darwin in northern

65   Australia. This site is representative of the dominant ecosystem of that region. Climate of this site is

66   typical of northern Australia with extremely seasonal and high rainfall and approximately 56% of this

67   site is burnt annually (Murphy *et al.*, 2010). However, in this study, data collected from Howard

68   Springs (approximately 65 km north of Litchfield SuperSite; (Cernusak *et al.*, 2011) have been used as

69   a representative of this particular SuperSite. This approach is justified because both of these sites

70   had very similar vegetation and climate conditions as well as frequency of occurrence of fire. The

71   stand structure in these two sites are sufficiently similar as to not shift physiological properties at

72   the leaf-scale given the species occurred in both sites largely overlap (Bowman *et al.*, 2001; Hutley

73   and Beringer, 2010; Murphy *et al.*, 2010).

74   **FNQ Rainforest**

75   The FNQ Rainforest SuperSite is located in a tropical wet forest ~140 km north of Cairns in Far North

76   Queensland. This SuperSite is structurally divided into two transects – a) the lowland rainforest

77   based in the Daintree rainforest near Cape Tribulation (MAT = 25.2 °C, Ozflux site average MAP =

78   5700 mm) and b) the upland rainforest based around Robson Creek (MAT = 21 °C, MAP = 2140 mm).

79   Precipitation is highly seasonal with most occurring during summer (Weerasinghe *et al.*, 2014). FNQ

80   supports 10% of Australian flora despite of occurring in only 0.2% its landmass. Consequently a

81   substantial number of the species in this study comes from this SuperSite. Data from two nodes of

82   this SuperSite, i.e., Cape Tribulation and Robson Creek were collected and analysed independently in

83   this study because of significantly different environmental clines (altitude, MAT and MAP) that exists
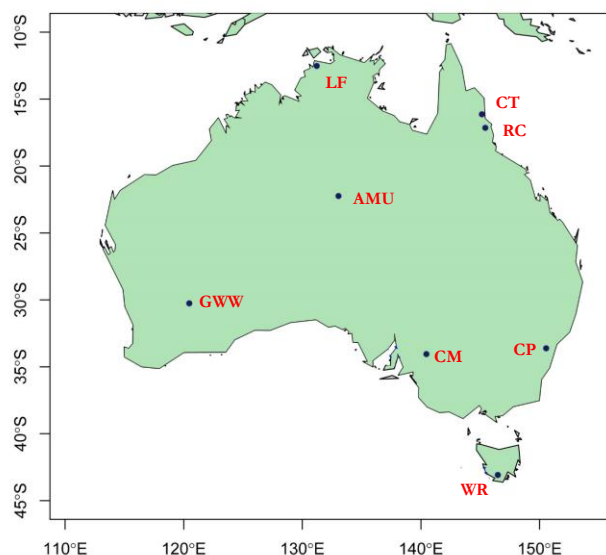
84   in these two nodes of FNQ.

85

86

Figure S1:   **Location of SuperSites (represented by black dots).**

88

89

90
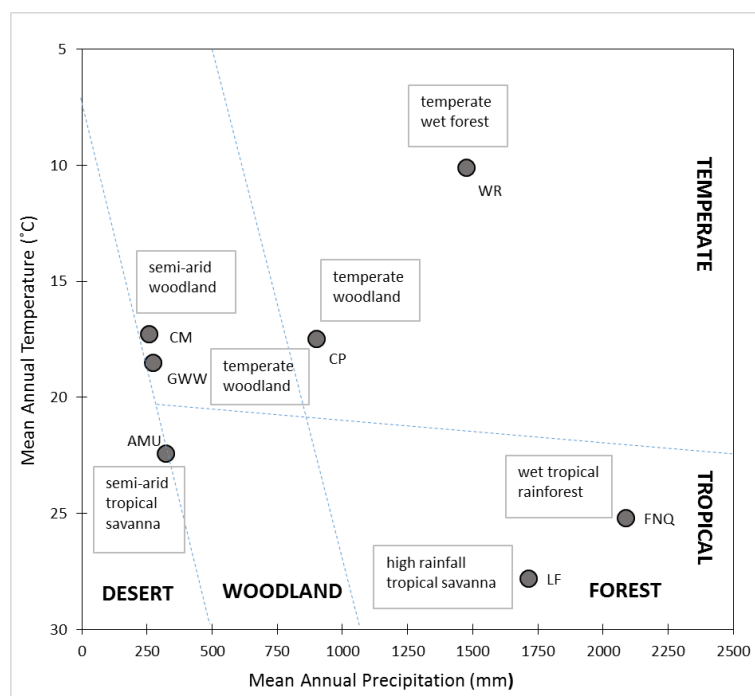**Figure S2:**   **Mean annual temperature, mean annual precipitation, and biomes of the study**
sites.
Each SuperSite is plotted in the Whittaker Biome Diagram (Whittaker, 1975) using the MAT
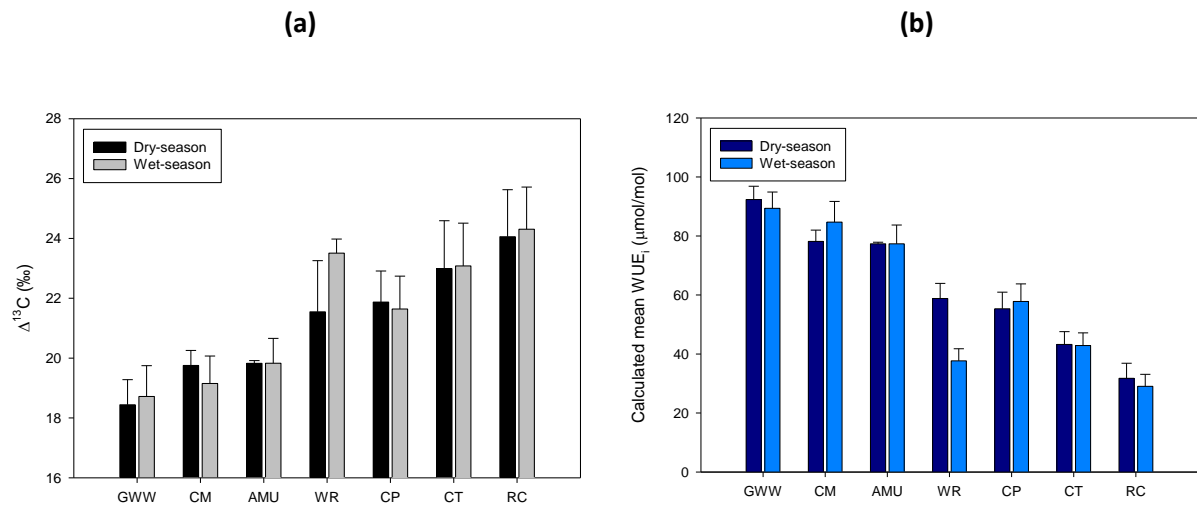and MAP observations generated for each site from the WorldClim data.

95

(a)

(b)

96　**Figure S3:**　　**Site mean values of (a) Δ^{13}C and (b) WUE$_i$**
97　　　　　　　Dark and light bars represent mean of dry and wet-season respectively and the error bars
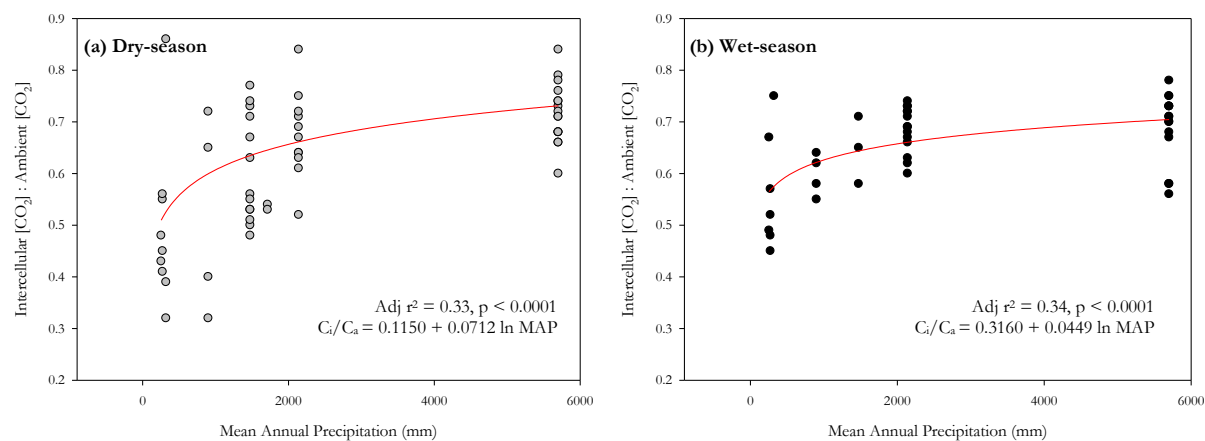98　　　　　　　represent standard errors.

Figure S4: Ratio between intercellular and ambient [CO$_2$] (C$_i$/C$_a$) for both seasons plotted as functions of mean annual precipitation (MAP).

Left and right panels are plotted from dry- and wet-season data respectively. Statistically significant correlations with MAP are plotted with red regression lines.
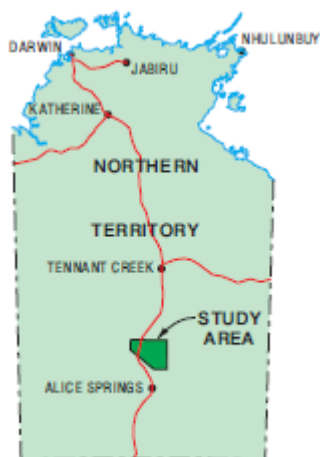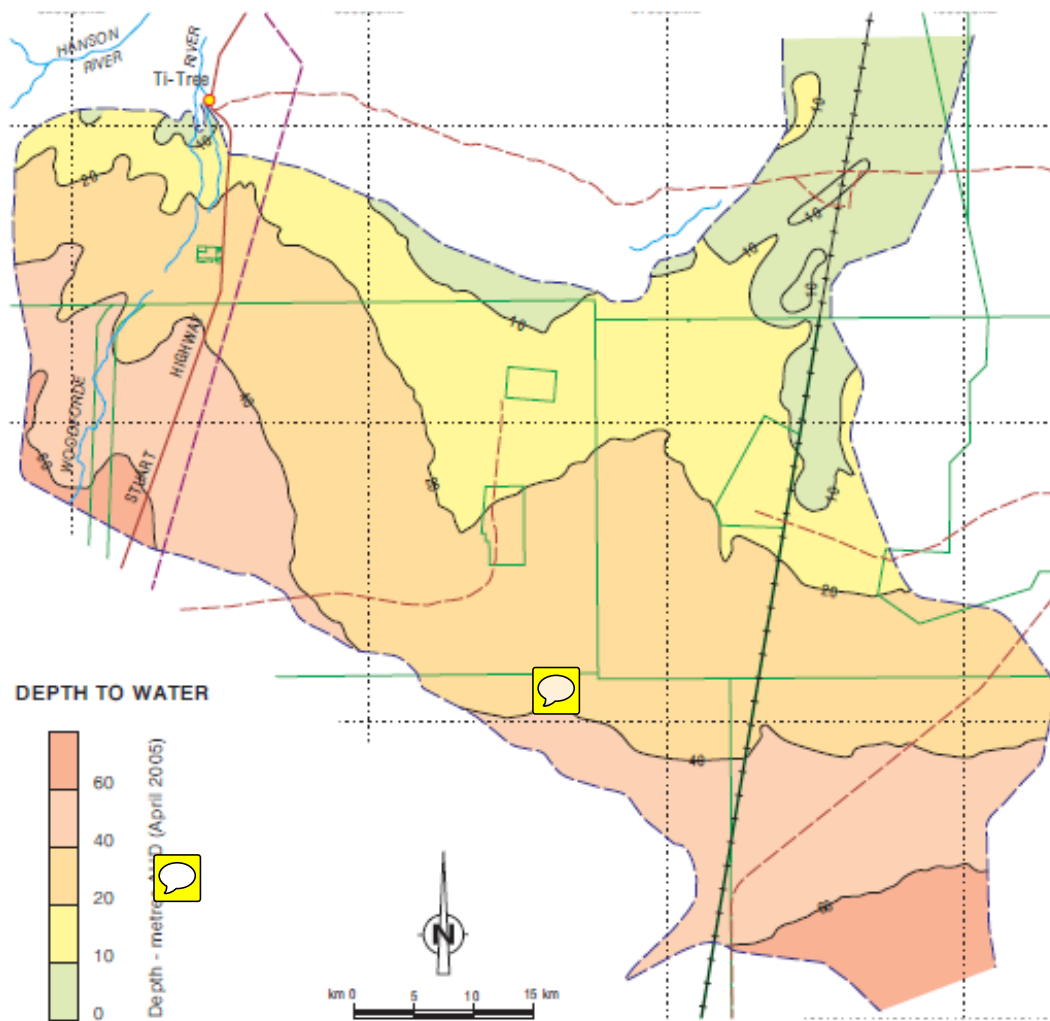
Figure S4: Map of the Northern Territory (NT) of Australia and the study area within the NT and the Ti Tree basin.